treated *mdx* mice.[9] These results indicate that rAAV-mediated microdystrophin transfer is a good therapeutic strategy for dystrophin deficiency.

For the application of our strategy to DMD patients, it is necessary to examine the therapeutic effects and the safety issue in larger animal models. To this end, we have recently established a colony of beagle-based canine X-linked muscular dystrophy in Japan ($CXMD_J$).[10,11] In contrast to moderate dystrophic changes of *mdx* mice, $CXMD_J$ show similar dystrophic phenotypes to those of human DMD: increased serum creatine kinase level, gross muscle atrophy with joint contractures, cardiomyopathy, prominent muscle necrosis, degeneration with mineralization and concurrent regeneration, and endomysial and perimysial fibrosis.[11,12] Therefore, affected dogs are useful for preclinical trials to predict the clinical effectiveness in DMD application. In addition, side effects of treatment modalities should be investigated in detail in the dog model to avoid unexpected, detrimental effects on DMD patients. For instance, human trial in hemophilia B was ineffective due to T-cell-mediated immunity to AAV capsid antigens, and represented the matter that further studies for immunomodulation in preclinical and human trials were required to achieve successful transduction.[13]

In this report, we demonstrate that rAAV2 efficiently infect canine myotubes and express the *lacZ* gene *in vitro*. In contrast, rAAV-mediated gene transfer into canine muscle *in vivo* elicits severe immune responses against the gene product, due to susceptive immune responses in the dog. These results suggest that it is important to know molecular backgrounds of immune response against AAV particles and its gene product in the host and consider immunosuppression in preclinical and clinical settings.

Results

rAAV2-CMVLacZ efficiently transduces canine primary myotubes in vitro

To investigate the transduction efficiency of a rAAV2 in canine muscle cells, we first infected primary myotubes prepared from C57BL/6 mice and wild-type beagle with rAAV type 2 encoding β-galactosidase (β-gal) driven by the CMV promoter (rAAV2-CMVLacZ) at doses from 2×10^8 to 2×10^{11} vector genomes (vg) (Figure 1). Surprisingly, more canine myotubes were β-gal-positive than murine ones. To enhance the transgene expression by converting single-strand viral DNAs into double-strand DNAs after the rAAV infection,[14] we next co-infected myotubes with helper adenovirus (Ad) and rAAV2. As expected, Ad enhanced the expression of *lacZ* in both murine and canine myotubes, but β-gal expression was much more robust in canine primary myotubes than in mouse primary myotubes.

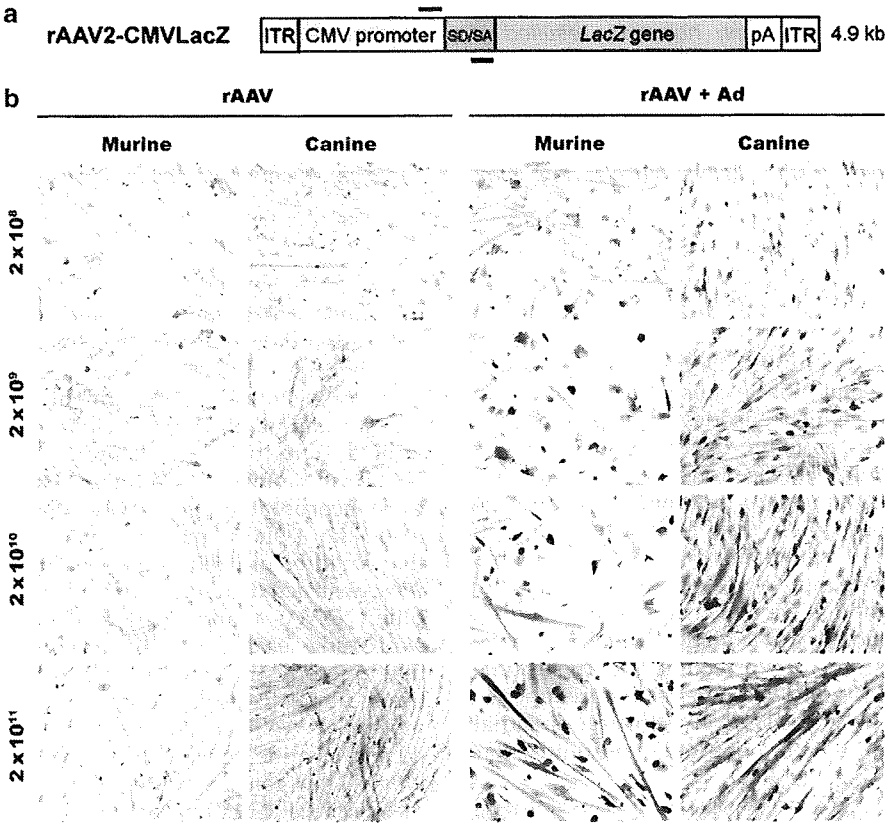

Figure 1 Successful transduction of a rAAV2 in murine or canine primary myotubes *in vitro*. (**a**) Diagram of rAAV2-CMVLacZ. Upper and lower bars correspond to primer positions used for detection of genome and mRNA in Figure 2b. SD/SA: splicing donor and acceptor. (**b**) *In vitro* infection assay of rAAV2-CMVLacZ in murine and canine primary myotubes. Myotubes were infected with serial doses (2×10^8–2×10^{11} vg/well) of rAAV2-CMVLacZ in the absence or presence of adenovirus (+Ad), and 2 days later β-gal expression was detected by X-Gal staining. Magnification: ×400. β-gal, β-galactosidase; X-Gal, 5-bromo-4-chloro-3-indolyl-β-D-galactopyranoside.

Low efficacy of gene transfer via rAAV into canine skeletal muscle in vivo

To examine the transduction efficiency of rAAV2 in canine myofibers *in vivo*, rAAV2-CMVLacZ was injected into skeletal muscles of wild-type beagles and golden retrievers at various ages, and β-gal expression in the rAAV-injected muscles were evaluated at 2, 4 and 8 weeks after the injection (Figure 2a and Table 1). We previously reported that intramuscular injection of the rAAV2 into normal mice permitted sustained β-gal expression for at least 8 weeks.[8] In contrast to the mice, however, a few β-gal-positive fibers were observed in canine muscles at 2, 4 and 8 weeks after the injection of rAAV2-CMVLacZ both in beagles and golden retrievers. Moreover, in the rAAV2-injected canine muscles, a large number of mononuclear cells were observed around β-gal-expressing fibers at 2, 4 and 8 weeks after the injection (hematoxylin and eosin (H&E) in Figure 2a, Table 1). rAAV injection at neonatal stage or administration of low dose of the rAAV resulted in a little prolonged

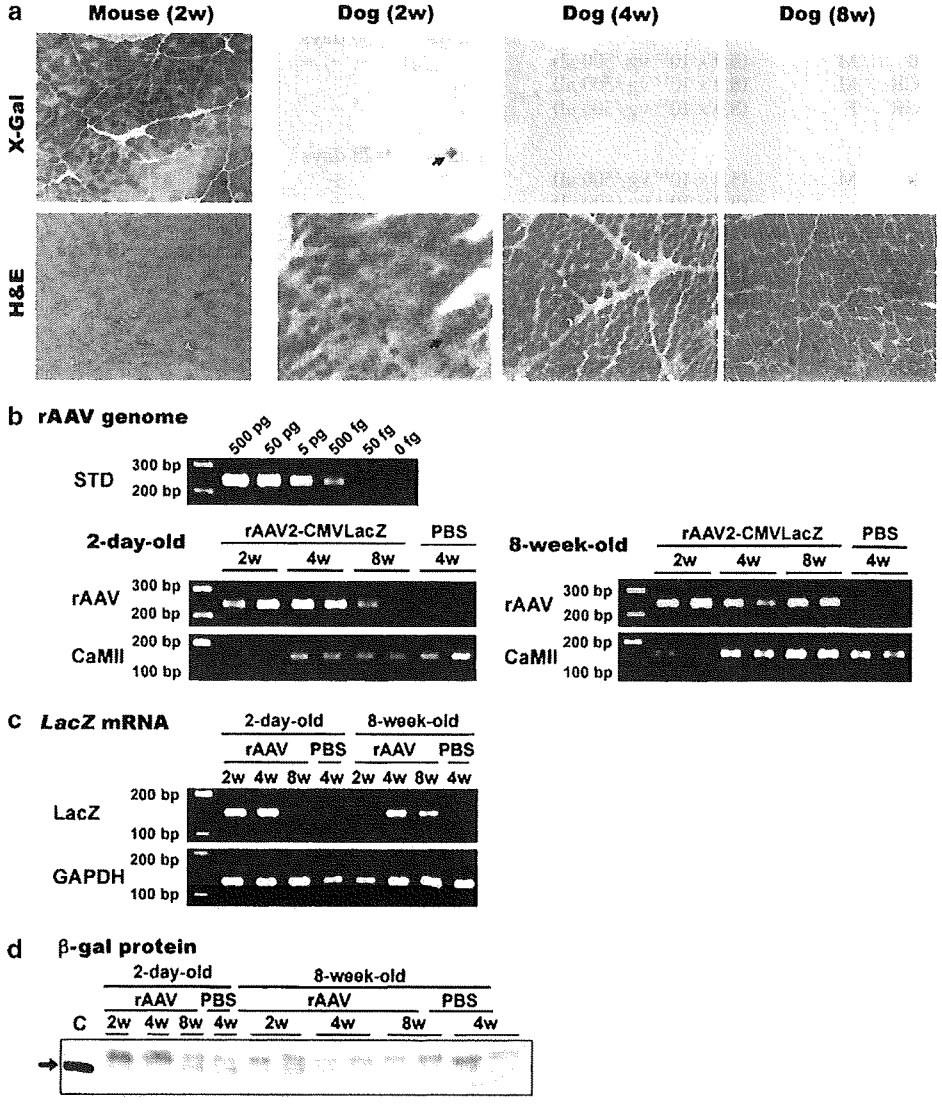

Figure 2 Low transgene expression and marked cellular infiltration after rAAV2-mediated gene transfer into canine skeletal muscle. rAAV2-CMVLacZ was injected into normal muscles of beagles or golden retrievers at various ages. (**a**) Representative images of β-gal expression and histological change in the rAAV-injected murine (TA) and canine muscles at 2, 4 and 8 weeks post-injection (left TA, right TA and right ECU muscles of dog FD89 in Table 1, respectively). The same batches of rAAV2-CMVLacZ were injected into murine and canine skeletal muscles. Identical parts of the serial cross-sections were shown in X-Gal and H&E stains. Large and widespread (2w), or scattered clusters (4w, 8w) of infiltrating cells were observed in the rAAV-injected canine muscles. Magnification: × 200. (**b**, **c** and **d**) Detection of rAAV genomes (**b**), transgene mRNA (**c**) and β-gal protein (**d**) in the canine muscles injected at 2 days (dogs: 3290 and 0665) and 8 weeks (dogs: 0338). Total DNA, RNA or protein was extracted from rAAV2-CMVLacZ- or PBS-injected muscles after 2, 4 and 8 weeks post-injection. Genome (244 bp) or mRNA sequences (178 bp) of the rAAV was amplified from 200 ng of template DNA or an aliquot of RNA by PCR or RT-PCR, respectively (**b**, **c**). STD: quantity standard of AAV vector plasmid; rAAV: rAAV2-CMVLacZ genome; LacZ: β-gal mRNA; CaMII and GAPDH: internal controls of genome and message. Muscle extracts (40 μg/lane) and control β-gal (lane c) were separated on a sodium dodecyl sulphate-polyacrylamide gel, and β-gal (arrow) was detected by western blotting (**d**). AAV, adeno-associated virus; β-gal, β-galactosidase; GAPDH, glyceraldehyde-3-phosphate dehydrogenase; H&E, hematoxylin and eosin; rAAV, recombinant adeno-associated virus; TA, tibialis anterior.

Table 1 Gene transfer of rAAV2-CMVLacZ into canine skeletal muscles

Animal[a]			*Injection*[b]	*β-Gal expression*[c]			*Cellular infiltration*[d]		
				2 weeks	*4 weeks*	*8 weeks*	*2 weeks*	*4 weeks*	*8 weeks*
Injection at 2 days				10 days	30 days	65 days	10 days	30 days	65 days
9223	GR	F	(8.2×10^{11} vg/100 μl)	±	–	–	±	±	±
3290	B	M	(1.5×10^{12} vg/100 μl)	–	±	–	+	++	+
7690	B	M	(1.5×10^{12} vg/100 μl)	±	±	–	+	++	±
0665	B	M	(2.2×10^{12} vg/100 μl)	±	–	–	+	++	±
Injection at 4 weeks				13d			13d		
7329	B	F	(1.0×10^{12} vg/100 μl)	–, –, –, –			+, +, +, +		
4657	B	F	(1.0×10^{12} vg/100 μl)	±, –			+, ±		
Injection at 8 weeks				10 days	30 days	59 days	10 days	30 days	59 days
02490	B	M	(5.0×10^{12} vg/500 μl)		–, –, –			++, ++, +	
0338	GR	M	(8.0×10^{12} vg/500 μl)	++	–	–	+	++	+
FD89	GR	F	(8.0×10^{12} vg/500 μl)	±	–	–	++	+	+
Injection at 10 weeks				14 days	28 days		14 days	28 days	
901[e]	B	M	(5.0×10^{10} vg/500 μl)	±	±		–	+	
			(5.0×10^{11} vg/500 μl)	–	±		–	++	
Injection at 12 weeks				10 days	30 days	59 days	10 days	30 days	59 days
FF04	GR	M	(8.0×10^{12} vg/500 μl)	±	–	–	++	+	±
E566	GR	M	(8.0×10^{12} vg/500 μl)	–	–	–	++	+	–
Injection at 16 weeks					27 days			27 days	
02232	B	M	(5.0×10^{12} vg/500 μl)		–, –, –			++, +, +	
Injection at 6 months				14 days			14 days		
0065	B	F	(7.5×10^{12} vg/500 μl)	±			+		
Injection at 14 months					28 days			28 days	
D01	B	M	(5.0×10^{11} vg/500 μl)		–, –, –			+, ±, +	
D03	B	M	(5.0×10^{12} vg/500 μl)		–, –, –			+, ++, ++	

[a]Canine species and sex: B, beagle; GR, golden retriever; M, male; F, female.
[b]Dosage per muscle: rAAV titer (vg) and injection volume (μl).
[c]β-Gal-positive fibers: –, 0; ±, <100; +, <300; ++, <1000; +++, >1000.
[d]Infiltrating cells: –, not detected; ±, few; +, moderate; ++, extensive.
[e]Two kinds of dosages of rAAV were injected into a dog.
In [c] and [d], individual results of the injected muscles were shown.

expression of the transferred gene (Table 1, dogs 3290, 7690 and 901). To determine whether contamination of cellular proteins in the stocks of AAV vectors lowers transduction efficiency, we tried three different AAV preparation protocols: (i) two-cycle CsCl density gradient ultracentrifugation, (ii) heparin column chromatography, or (iii) combination of them, and found that preparation using heparin column chromatography showed high levels of contamination of transgene products and cellular proteins (Supplementary Figure 1). CsCl ultracentrifugation efficiently eliminated contaminated empty viral particles. Combination of these two methods almost completely eliminated contaminated proteins. Nevertheless, all rAAV stocks showed high levels of β-gal expression in murine muscles (data not shown), but evoked cellular infiltration in normal canine muscles (Supplementary Figure 1).

To quantify the levels of infection and transduction of rAAV2-CMVLacZ in canine muscles, we isolated DNA and RNA from the injected muscles, and semiquantitatively evaluated rAAV genome copy numbers and the level of β-gal mRNA by PCR and reverse transcription (RT)-PCR, respectively. AAV vector genomes and β-gal mRNA were detected at 2, 4 and 8 weeks after the injection (Figures 2b and c). β-Gal protein, however, could not be detected by western blot at all stages after the injection (Figure 2d). These results suggest that canine myofibers were transduced by a rAAV2 *in vivo*, but the transduced cells were eliminated by the host's defense mechanisms.

rAAV-mediated gene transfer into canine muscles evoke both cellular and humoral immune response

We next analyzed cell markers on infiltrating cells in the rAAV2-CMVLacZ-injected muscles (Figure 3a) at 2 weeks after the injection at 12 weeks. Numerous CD4+ or CD8+ T lymphocytes were detected in the interstitial spaces of the injected muscle. CD11b+ cells and B cells were also detected in the cluster of infiltrating cells. Furthermore, the expression of the major histocompatibility complex (MHC) class I and -II molecules were highly upregulated on both mononuclear cells and muscle fibers. IgG deposits were found in both the

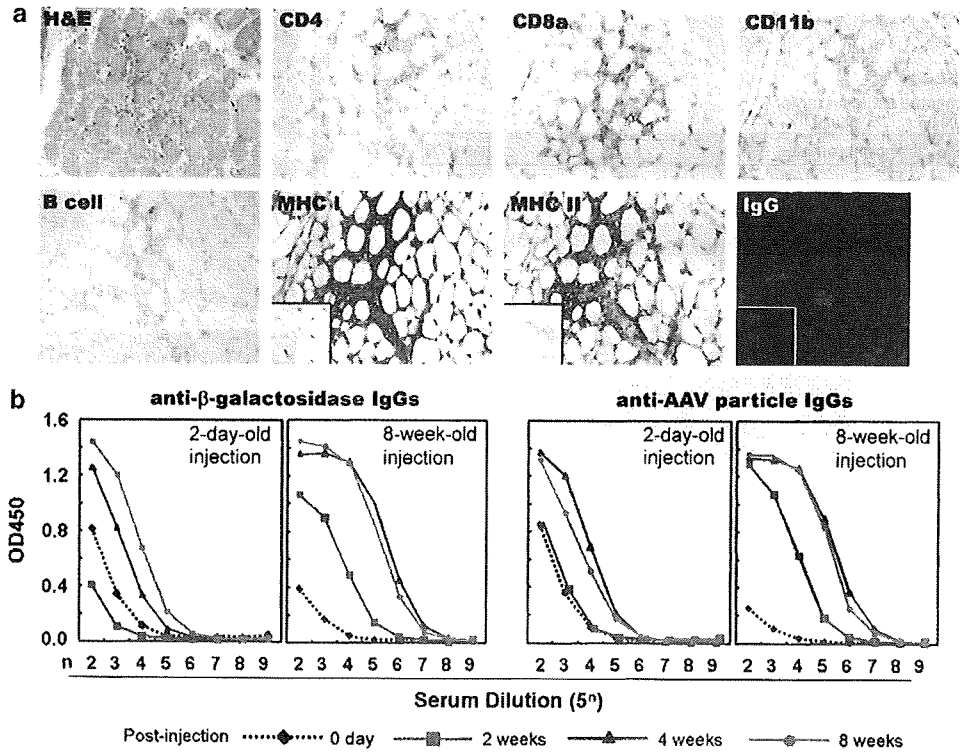

Figure 3 Immune responses were remarkably activated after rAAV2-mediated gene transfer into canine muscles. (**a**) Infiltrating cells in the rAAV2-CMVLacZ-injected canine TA muscles at 2 weeks after the injection. Serial cross-sections were immunostained with antibodies against canine CD4, CD8a, CD11b, B cell, MHC class I and -II, and IgGs. Insets show the noninjected muscles. Dog: FF04. Magnification: ×400. (**b**) Humoral immune responses against the transgene product and rAAV particle in the rAAV-treated dogs. Sera from dogs injected with rAAV2-CMVLacZ at 2 days and 8 weeks were analyzed for the presence of IgG antibodies against β-gal or AAV particle at 0, 2, 4 and 8 weeks after the injection, using ELISA. Dogs: 9223 and 0338. AAV, adeno-associated virus; β-gal, β-galactosidase; ELISA, enzyme-linked immunosorbent assay; MHC, major histocompatibility complex; rAAV, recombinant adeno-associated virus; TA, tibialis anterior.

cytoplasm of myofibers and the extracellular space in the rAAV-injected muscle. We next examined the antibodies against the transgene product or rAAV particles in the sera of rAAV-injected dogs (Figure 3b). The levels of serum IgGs that react β-gal protein or rAAV2 particle were gradually increased with time in both 2-day-old and 8-week-old injections. When injected at 8 weeks, the levels of IgGs against β-gal or rAAV2 increased from 2 weeks after the injection, and reached the peak at 4 weeks. When injected at 2 days, anti-β-gal or anti-AAV antibodies were not detected at 2 weeks after the injection, but had begun to increase at 4 weeks. The results would explain why the lacZ was expressed for a longer time, when injected at neonatal age (Table 1). These results suggest that cellular and humoral immune responses are elicited after the transfer of a rAAV2 into canine muscles.

Administration of a rAAV expressing no transgene into canine muscles

Transduction of skeletal muscle by rAAV2-CMVLacZ presents two main foreign antigens, namely β-gal protein and AAV capsid to the host's immune system. To test which antigen is responsible for rapid elimination of transduced myofibers after rAAV-mediated gene transfer into canine muscle, we constructed a rAAV2 expressing no transgene, named rAAV2-LacZ-P(−), by removing the MCK promoter from the parental rAAV2-MCKLacZ (Figure 4a). We confirmed that the promoter-deleted rAAV2 expressed no β-gal in muscle after injection into skeletal muscles of normal mice (5×10^{11} vg/50 μl/site) (data not shown). Then, we injected the same titers of rAAV2-LacZ-P(−) and rAAV2-CMVLacZ, into skeletal muscles of normal adult beagles, and evaluated transduction efficiency by quantitative PCR of AAV genomes or histopathologically at 2 and 4 weeks post-injection. In 5 × 5 × 10 mm tissues of rAAV2-LacZ-P(−)-injected muscles, 1–10 pg of rAAV genomes were detected by PCR, whereas 500 fg to 5 pg of rAAV sequences were amplified in the injected muscles of rAAV2-CMVLacZ (Figures 2b and 4b). These results indicate that the promoter-deleted rAAV2 could successfully infect canine muscles and the viral genomes were retained stably in the fibers.

H&E staining showed that deletion of the MCK promoter greatly reduced the cellular infiltration into the rAAV2-LacZ-P(−)-injected muscles at 2 and 4 weeks after the injection, in contrast to the rAAV2-CMVLacZ-injected muscles (Figure 4). Even in a muscle sample in which vector genome was detected at the highest level by PCR, infiltrating cells were rarely found (sample 1c in Figures 4b and c). In addition, CD4+ or CD8+ cells were not detected in the rAAV2-LacZ-P(−)-injected muscles (data not shown). These results suggest that the transgene product but not AAV particle strongly elicits immune responses that subsequently eliminated transduced myofibers.

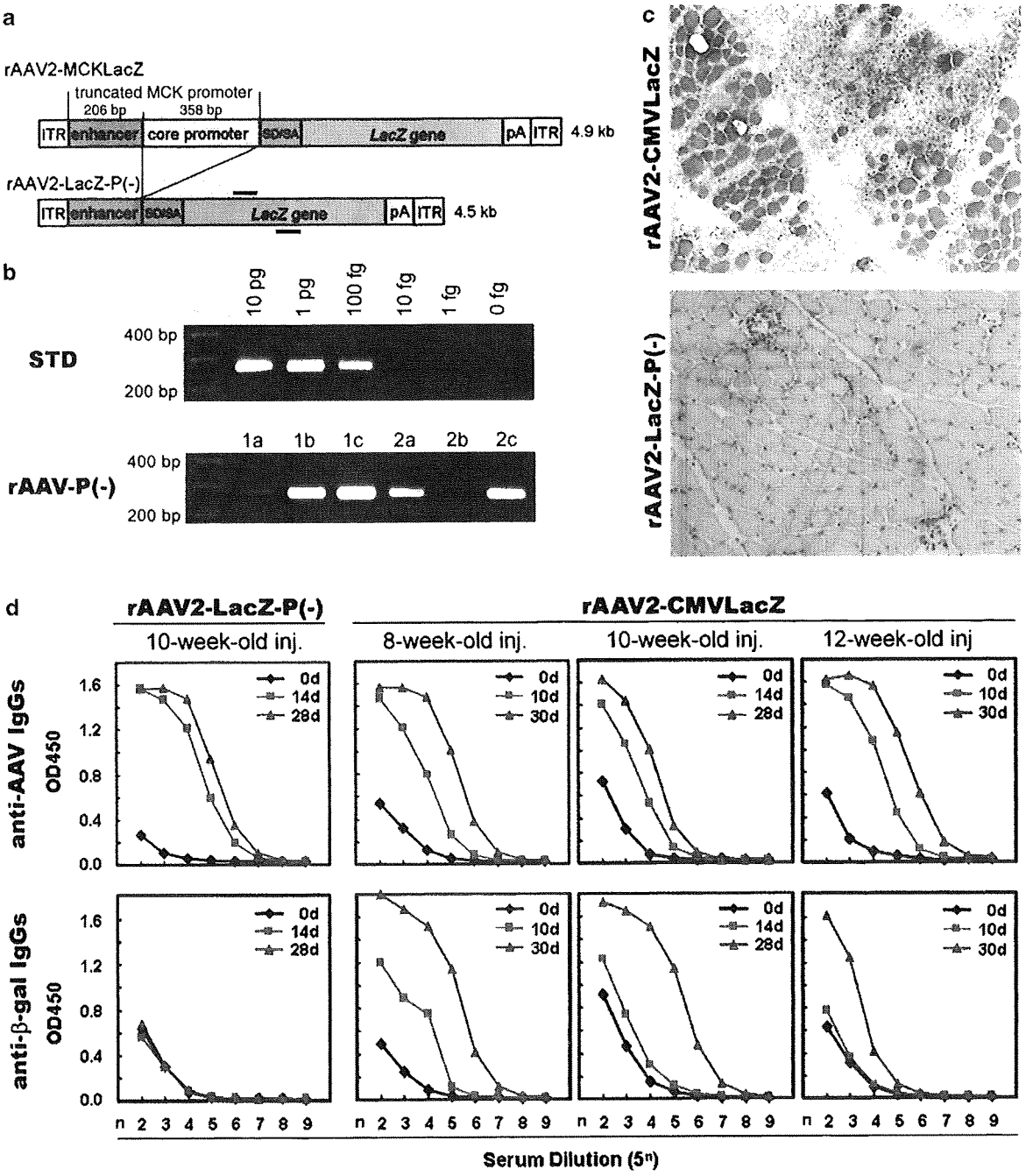

Figure 4 Injection of the promoter-deleted rAAV2 showed negligible cellular infiltration in canine muscle. The promoter-deleted rAAV2, rAAV2-LacZ-P(−) (5×10^{12} vg/500 μl/site) was injected into skeletal muscles of 10-week-old beagle (dog 902), and the injected muscles and sera were analyzed at 2 and 4 weeks post-injection. (**a**) Schematic illustration of rAAV2-LacZ-P(−). Upper and lower bars correspond to primer positions used for detection of genome in Figure 4b. (**b**) Detection of rAAV genome DNA in the rAAV-LacZ-P(−)-injected canine muscles. Total DNA was extracted from the muscle sections, and *LacZ* DNA fragment (275 bp) was amplified from 200 ng of template DNA by PCR. Results at 2 weeks after the injection were shown. The numbers 1a–2c show individual identities of the muscle specimen divided into pieces. Vector genomes were detected in all samples, but amplified levels were different between muscle blocks. STD: quantity standard of AAV vector plasmid; rAAV-P(−): rAAV2-LacZ-P(−) genome. (**c**) Cellular infiltrations were rarely observed in the rAAV2-LacZ-P(−)-injected canine TA muscle (sample 1c). Canine muscles were injected with the rAAVs expressing β-gal or no transgene, and the muscle blocks were sectioned and stained with H&E staining at 2 weeks after the injection. All muscle samples from rAAV2-CMVLacZ (1a–2c) showed minimal cellular infiltration. Magnification: ×200. (**d**) Detection of antibodies against AAV particles and β-gal in the rAAV-treated dogs. Sera from dogs injected with rAAV2-LacZ-P(−) (dog 902) or rAAV2-CMVLacZ (dogs 0338, 901 and FF04, also see Table 1) were analyzed by using the ELISA technique for the presence of IgG antibodies against AAV particles and β-gal protein at 0, 2 and 4 weeks after the injection. AAV, adeno-associated virus; β-gal, β-galactosidase; ELISA, enzyme-linked immunosorbent assay; rAAV, recombinant AAV.

Next, we measured the anti-AAV IgG type antibodies in the serum of the treated dogs (Figure 4d). In the rAAV2-LacZ-P(−)-injected dog at 2 and 4 weeks after the injection, anti-AAV2 antibodies were detected at high levels similar to those in rAAV2-CMVLacZ-injected dogs, but antibodies against β-gal were undetectable. This indicates that antibodies against AAV particles were developed in rAAV2-LacZ-P(−)-injected dogs but did not lead to elimination of transduced cells.

Immunosuppression of the rAAV-injected dogs slightly improved the expression of the transgene

To test whether immunosuppression could improve transduction by rAAV-2 in canine muscle, we daily administered cyclosporine to the rAAV2-CMVLacZ-injected dogs from −5 day of the injection until the sampling day of muscle specimens (Table 2A). Unexpectedly, β-gal expression in the injected muscles of cyclosporine-treated dogs was as low as that in the untreated dogs. Only the extensor digitorum longus (EDL) muscle of dog 403 expressed β-gal at a high level at 2 weeks after the injection, although a large number of infiltrating cells with CD4+ or CD8+ cells and upregulation of MHC class I and -II were detected (data not shown). In contrast, in the rAAV2-CMVLacZ-injected extensor carpi ulnaris (ECU) muscle of dog 403 at 2 weeks post-injection, β-gal expression was much lower than that in the EDL muscle. Thus, as a whole, cyclosporine alone could not effectively improve transduction of rAAV2-CMVLacZ.

Mycophenolate mofetil (MMF) suppresses the functions of T lymphocytes in a different way with cyclosporine. Therefore, to suppress immune responses more effectively, we treated the rAAV2-CMVLacZ-injected dogs both with MMF and cyclosporine. MMF was daily administrated from 0 day to the day of sampling (Figure 5 and Table 2B). This combined immunosuppression significantly increased the numbers of β-gal-expressing fibers, compared with those in the untreated muscles when examined at 2 weeks after the injection, but cellular infiltration was still observed. Some CD4+ or CD8+ cells and upregulation of MHC class I and -II in infiltrating cells and myofibers were detected in rAAV2-CMVLacZ-injected muscle (data not shown). After 4 weeks, β-gal expression significantly decreased together with increasing infiltrating cells. These results indicated that combination of cyclosporine and MMF could partially improve the transduction efficiency of a rAAV2 in canine muscles.

Immunological background of enhanced immune responses in dogs

We next investigated possible differences in immune responses between mice and dogs, which might explain why rAAV2 injection evoked strong immune responses in canine muscles. To this end, we prepared single-cell suspension from spleens of untreated dogs or mice, stimulated them with AAV capsids and purified β-gal protein *in vitro*, and assayed the secretion of interferon-γ (IFN-γ) by enzyme-linked immunosorbent assay (ELISA; Table 3). We also stimulated the splenocytes with two major mitogens for T lymphocytes, concanavalin A (ConA) and phytohemagglutinin (PHA). When stimulated with ConA or PHA, canine splenocytes secreted much larger amount of IFN-γ into the culture medium than murine cells. Furthermore, canine cells secreted slightly higher levels of IFN-γ in response to β-gal or rAAV2 capsid proteins than murine cells. These results suggest that canine splenocytes are innately more susceptive to

Table 2 Gene transfer of rAAV2-CMV-LacZ into canine skeletal muscles under immunosuppression

Animal[a]			*Injection*[b]	*Cyclosporine*	*Expression*[c]		*Infiltration*[d]	
(A) Cyclosporine alone								
Injection at 5 weeks				Dose/kg/day	2 weeks	4 weeks	2 weeks	4 weeks
601	B	M	(6.0×10^{12} vg/500 μl)	20 mg	−		+	
Injection at 8 weeks								
1103	B	M	(5.0×10^{10} vg/500 μl)	25 mg	−, −	±, −	±, ±	+, −
1102	B	M	(6.0×10^{11} vg/500 μl)	25 mg	±, −	±, −	+, ±	+, +
Injection at 11 weeks								
403	B	M	(7.7×10^{12} vg/500 μl)	20 mg	+++, +[e]	+, ±	+, +	+, +
703	B	M	(5.0×10^{12} vg/500 μl)	50 mg	−		±	
Animal[a]			*Injection*[b]	*Cyclosporine, MMF*	*Expression*[c]		*Infiltration*[d]	
(B) Cyclosporine and MMF								
Injection at 10 weeks				Dose/kg/day	2 weeks	4 weeks	2 weeks	4 weeks
VC1XE	B	M	(5.0×10^{11} vg/500 μl)	25 mg, 30 mg	++, +	±, +	+, ±	+, ++
TC2XE	B	M	(5.0×10^{12} vg/500 μl)	25 mg, 30 mg	±, +	+, −	+, +	++, +
Injection at 12 weeks								
1902	B	M	(5.0×10^{11} vg/500 μl)	25 mg, 30 mg	+	++	±	±

Abreviations: B, beagle; ECU, extensor carpi ulnaris; EDL, extensor digitorum longus; F, female; M, male; MMF, mycophenolate mofetil.
[a–d]See Table 1.
[e]+++ was seen in an EDL muscle, whereas + was in an ECU muscle.
In [c] and [d], individual results of the injected muscles were shown.

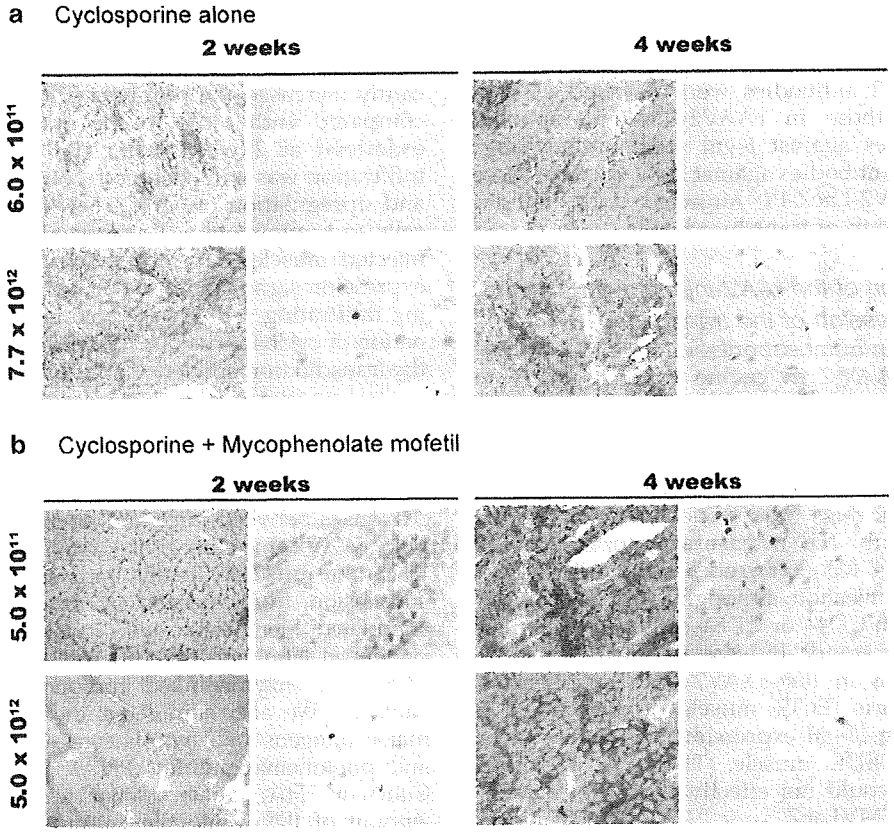

Figure 5 Combined immunosuppression partially improved transgene expression in rAAV2-mediated gene transfer into canine muscle. Representative H&E and X-gal stainings showing improvement in the transduction efficiencies of rAAV2-CMVLacZ at 2 and 4 weeks after the injection under immunosuppression (also see Table 2). The rAAV (5.0×10^{11}–7.7×10^{12} vg/site) was injected into TA and ECU muscles of beagles, and the dogs were daily treated with cyclosporine alone (**a**) or combination of cyclosporine and MMF (**b**). The muscle of dog 1102 was injected with rAAV at a dose of 6.0×10^{11} vg (upper panels in **a**). Dog 403 was injected with rAAV at a titer of 7.7×10^{12} vg; beagle VC1XE was injected with rAAV at a dose of 5.0×10^{11} vg (upper panels in **b**). TC2XE was injected with 5.0×10^{12} vg rAAV (lower panels in **b**). Magnification: $\times 100$. ECU, extensor carpi ulnaris; H&E, hematoxylin and eosin; MMF, mycophenolate mofetil; rAAV, recombinant adeno-associated virus; TA, tibialis anterior; X-gal, 5-bromo-4-chloro-3-indolyl-β-D-galactopyranoside.

immunogens or mitogens than murine ones, and this immunological difference might underlie severer immune responses to rAAV2 injection in dogs than in mice.

Discussion

rAAV2 drives a long-term expression of microdystrophin genes in skeletal muscles of dystrophic mice,[9] therefore it is an attractive tool for treatment of DMD. To test the efficacy and safety of rAAV-mediated gene transfer into skeletal muscle of larger animal models, we directly injected rAAV2 encoding β-gal into skeletal muscle of normal dogs and examined the β-gal expression at several time points. Unexpectedly, we found that rAAV2-mediated gene transfer elicits strong immune responses against the transgene product in canine skeletal muscles. The mechanisms of enhanced immune reactions after rAAV2 injection seen in normal dogs need to be clarified before applying rAAV-mediated gene therapy to boys with DMD.

rAAV2 efficiently transduces canine muscle in vitro *but not* in vivo

In mice, β-gal expression is maintained for a long time after rAAV-CMVLacZ injection into muscle.[8] In contrast, low levels of β-gal expression and numerous infiltrating cells were observed in the rAAV2-CMVLacZ-injected canine muscle. Surprisingly, rAAV2 infected and transduced canine myotubes more effectively than murine myotubes *in vitro* (Figure 1). Therefore, we conclude that the low expression of the transgene in dog muscle is not due to the lack of receptors for the AAV2 on canine muscle fibers.

Cytotoxic immune response against the transgene product

Immunosuppression reduced cellular infiltration in rAAV2-CMVLacZ-injected muscle and partially rescued the β-gal expression in myofibers, suggesting that cytotoxic T-cell responses to transduced muscle fibers are largely responsible for the elimination of β-gal-positive myofibers in the injected muscle. Furthermore, intramuscular injection of the promoter-deleted rAAV2, which can infect the muscle (Figure 4) but express no β-gal (data not shown), induced much less cellular infiltration in canine muscle than the rAAV2-CMVLacZ. This observation suggests that massive destruction of the transduced muscle cells is mainly due to cellular immunity against the transgene product but not against AAV capsid proteins.

Table 3 IFN-γ release assay in murine and canine splenocytes

Immunogen		*IFN-γ (pg/ml)*	
		Mouse	*Dog*
None	—	<9.4	<32
β-gal	500 ng	<9.4	<32
	5 μg	<9.4	166±5
	50 μg	334±20	1316±122*
rAAV	1×10^8 vg	<9.4	<32
	1×10^9 vg	<9.4	<32
	1×10^{10} vg	<9.4	59±19
ConA	5 ng	<9.4	<32
	50 ng	<9.4	4928±162
	500 ng	6750±132	57 567±6374*
	5 μg	4095±474	65 050±5467*
PHA	50 ng	<9.4	49±7
	500 ng	<9.4	5227±479
	5 μg	2683±253	43 833±4488*
	50 μg	5453±349	60 133±6616*

Abbreviations: β-gal, β-galactosidase; ConA, concanavalin A; ELISA, enzyme-linked immunosorbent assay; IFN-γ, interferon-γ; PHA, phytohemagglutinin; rAAV, recombinant adeno-associated virus.
Splenocytes were stimulated with various doses of immunogens, such as β-gal, rAAV particle (rAAV), ConA and PHA, and secreted level of murine and canine IFN-γ in culture medium were measured by ELISA. Data are expressed as means±s.d., and significant differences (*$P<0.01$) between mouse and dog were shown.

There have been several papers reporting studies of rAAV-based gene transfer into canine skeletal muscle. Most of them were gene transfer studies for hemophilia B dogs, and reported that cellular immune responses against Factor IX, were nearly absent in dog models of hemophilia B.[15–19] The difference between studies of hemophilia and ours might be explained by the antigenicity of the transgene products. When we injected rAAV2-CMVM3 expressing M3 microdystrophin[7] into skeletal muscles of normal dogs, cellular infiltration was considerably reduced (data not shown), indicating that lowering the immunogenicity of therapeutic genes is important to improve the efficiency of gene therapy. In addition, nonsecreted, intracellular proteins might tend to evoke cellular immunity, compared with secreted proteins, like Factor IX.

We showed quite low expression of β-gal in rAAV2-CMVLacZ-injected muscle, whereas AAV genome and *LacZ* mRNA in rAAV-CMVLacZ-injected muscle were detected even at 8 weeks after the injection (Figure 2). The gap between *LacZ* mRNA level and β-gal protein cannot be fully explained at present. This might be simply due to time lag between transcription and translation of the transgene, or translation of β-gal might be repressed in inflammatory muscles.

Immunity against AAV2 capsid in dogs and humans

Promoter-deleted rAAV2 injection did develop antibodies against the AAV2 capsid after the injection into the skeletal muscle (Figure 4d), but did not evoke strong immune reactions in muscle, suggesting that cytotoxic T cells targeting the AAV2 capsid protein were not or minimally activated. This observation is consistent with the previous reports that cellular immune response to the AAV capsid was absent in hemophilia B dogs.[17–19] However, it is still unclear whether cellular immune response against the AAV2 capsid proteins is completely absent in dogs. Because even a low-level response could be problematic in the clinic, immunity to the AAV2 capsid proteins should be carefully monitored in dog models. In contrast, it has been recently reported that liver-directed rAAV2 transfer for human trial of hemophilia B led to destruction of transduced hepatocytes by cell-mediated immunity targeting the AAV2 capsid.[13] The authors suggest that T-cell immunity against the AAV2 particles might be associated with peptide sequence within the AAV2 capsid which had a high predicted binding potential to *B*0702* molecule of human MHC class I. This may explain why cell-mediated immune response against the AAV2 capsid protein was activated in humans.

Backgrounds of immune responses in dogs and mice

We measured the levels of IFN-γ secreted from canine or murine splenocytes after stimulation with β-gal, rAAV2 viral particles, ConA or PHA *in vitro*. Although biological activities (e.g., EC_{50}) of canine IFN-γ might be different from those of murine IFN-γ, it is likely that canine immune system is more sensitive to foreign antigens, such as β-gal. We also showed that canine splenocytes secrete much larger quantity of INF-γ than murine splenocytes when exposed to ConA or PHA. The higher levels of overall immune activation in dogs than in mice might be responsible for rapid development of immune response to rAAV2-mediated gene transfer into canine skeletal muscle, and might be partly explained by the different sanitary status of murine and canine colonies.

Antigen-presenting cells (APCs) in skeletal muscle play an important role in development of immunity to transgene products.[8,20] Therefore, it is also possible that rAAV transduces APCs more efficiently in dogs than in mice.

Threshold hypothesis for detrimental immune reaction

A previous study showed that systemic delivery of rAAVs, such as isolated limb perfusion (ILP) elicited less immune response than local injection.[19] Other study in hemophilia B dogs suggested that local Factor IX antigen dose in rAAV-injected muscles would be a critical parameter for risk of developing neutralizing antibody in dog.[18] The authors discussed that vector dose of 2×10^{12} vg/site and 8.5×10^{12} vg/kg might represent a threshold at which an inhibitory anti-Factor IX was or was not induced. These observations might indicate that the local concentration of the rAAV particles and its gene product is an important factor for establishment of immunity against rAAVs. Direct injection of rAAV2-CMVLacZ particles into muscle might cause the excessive expression of β-gal within a small area, and thereby mount strong cellular immune responses against gene products. Recently, we observed that pseudo-typed rAAV2/8 efficiently delivered the transgene into canine muscle (Ohshima *et al.*, unpublished observation). The expression of β-gal from rAAV8-CMVLacZ distributed more widely, and more evenly within the muscle than rAAV2-CMVLacZ after direct injection into canine

muscle. We hypothesize that widespread transduction of myofibers at a low dose of a rAAV2/8 could escape the establishment of immunity against the transgene products. New serotypes of AAVs, such as AAV8 or AAV9 can deliver the transgene into musculature of the whole body via circulation.[21,22] These vectors might overcome the immunological problems that we encountered in rAAV2-mdiated gene transfer into canine muscles.

In conclusion, we found that intramuscular administration of rAAV2-CMVLacZ elicited rapid and severe immune responses against the transgene product in wild-type dogs. This has not been observed in mice. It is important to understand well the mechanisms of immune reactions observed in dogs to circumvent immunological limitations, which might stand in our way in preclinical and clinical trials for DMD.

Materials and methods

Construction and production of rAAVs

We used rAAV2-CMVLacZ and rAAV2-CMVM3, which harbors the *Lac*Z gene or microdystrophin M3 driven by the CMV promoter, respectively.[3,7,8] To improve the expression efficiency of the LacZ gene in rAAV2-CMVLacZ, a chimeric intron (human β-globin splicing donor and immunoglobulin splicing acceptor, Promega, Madison, WI, USA) is inserted between CMV promoter and the LacZ gene.[8] rAAV2-LacZ-P(−) was generated by deleting the truncated MCK promoter (358 bp) from rAAV2-MCKLacZ, leaving the MCK enhancer intact.[8] We confirmed that rAAV2-LacZ-P(−) could not express β-gal in murine muscle cells both *in vitro* and *in vivo* (data not shown). The rAAV was produced by a plasmid triple-cotransfection method,[23] purified by two CsCl density gradient centrifugations[24] and/or heparin column chromatography,[25] and titrated by a quantitative DNA dot-blot assay.

Administration of rAAVs into canine or murine skeletal muscles and isolation of the injected muscles

Experimental dogs were wild-type littermates of beagle-based CXMD$_J$ breeding colony at National Center of Neurology and Psychiatry (NCNP; Tokyo, Japan),[10,11] or golden retriever muscular dystrophy colony at Murdoch University (Perth, Australia).[26] All animals were cared and treated in accordance with the guidelines approved by Ethics Committee for Treatment of Laboratory Animals at NCNP or Animal Ethics Committee at Murdoch University, where three fundamental principles (replacement, reduction and refinement) were also considered. When a rAAV was injected into dogs, the animals were not vaccinated to relive influences of immune response by vaccination. rAAVs were injected intramuscularly at ages from 2 days to 14 months, and the muscles were isolated after 2, 4 and 8 weeks. Surgeries were done under anesthesia with isoflurane, as described previously.[27] Briefly, the ECU, tibialis anterior (TA) or EDL muscles were surgically exposed and two marker sutures were placed on the mid-belly of the muscle at proximal and distal positions apart approximately 20 mm. rAAV (5×10^{10}–8×10^{12} vg in 100 or 500 μl) or phosphate-buffered saline (PBS) was injected slowly into the muscles between two markers along the length. In biopsy and necropsy, the entire muscle blocks with two sutures were removed, divided into some pieces, and immediately frozen in isopentane precooled with liquid nitrogen. rAAV (5×10^{11} vg/50 μl) was also injected into TA muscles of C57BL/10 mice at 5 weeks, and the muscles were isolated at 2 or 4 weeks after the injection.

Immunosuppression

To suppress immune reaction, we treated rAAV-injected dogs with cyclosporine alone or cyclosporine combined with MMF for immunosuppression. Cyclosporine (NEORAL capsules; Novartis, Basel, Switzerland) was administrated orally at doses of 20–50 mg/kg/day and daily from −5 day of the injection. MMF (CellCept capsules, Roche Pharmaceuticals, Nutley, NJ, USA) was administrated orally at a dose of 30 mg/kg/day and daily from 0 day of the injection.

Histological and immunohistochemical analysis

Transverse cryosections from the rAAV-injected muscles were stained with H&E or 5-bromo-4-chloro-3-indolyl-β-D-galactopyranoside (X-Gal).[8]

Immunohistochemistry was performed as described previously.[8] Cryosections were incubated with the following antibodies: mouse monoclonal antibodies against canine CD4 (CA13.1E4, Serotec, Oxford, UK), canine CD8a (CA9.JD3, Serotec), canine CD11b (CA16.3E10, Serotec), canine B cells (CA2.1D6, Serotec), class I major histocompatibility antigen (H58A, VMRD, Pullman, WA, USA) and canine MHC class II (CA2.1C12, Serotec), and fluorescein-conjugated goat affinity-purified antibody to dog IgG (whole molecule) (Cappel, Solon, OH, USA). The primary antibodies were detected using VECTASTAIN ABC kit (Vector Laboratories, Burlingame, CA, USA), then visualized with diaminobenzidine, and counterstained with methyl green.

In vitro *infection assay in primary myotubes*

Canine or murine primary myoblasts were isolated and differentiated into myotubes, according to the previously published protocol[28] with some modifications. Briefly, muscle mass was removed from dogs or mice at 0 day to 2 weeks, weighted and minced. Cells were enzymatically dissociated in PBS (4 ml per g of tissue) containing dispase II (2.4 IU/ml, Godo Shusei, Tokyo, Japan) and Collagenase type XI (0.2%, Sigma, St Louis, USA), and 2.5 mM $CaCl_2$. The slurry was incubated at 37°C for 90–120 min with trituration every 15 min, and then passed through 100 μm pore mesh. The filtrate was spun at 350 *g*, and the pellet was resuspended in growth medium (F-10 medium with 20% fetal bovine serum (FBS) and 2.5 ng/ml human basic fibroblast growth factor (Sigma)). The cell suspension was then plated on non-coated dishes for 90 min, and non-adherent cells were collected and plated onto new dishes. After several repeats of this pre-plating procedure, myoblasts were enriched. To assess transduction efficiency of a rAAV in primary myotubes, the same numbers of myoblasts (2×10^4 cells/well) were plated onto 24-well plates and maintained for a few days in differentiation medium (Dulbecco's modified Eagle's medium with 5% FBS and 10 μg/ml human insulin (Sigma)), and then cultured in the presence of rAAV2-CMVLacZ (2×10^8–2×10^{11} vg/well), or co-infected with the rAAV2 and adenovirus Ad5-dlX[3]

(1×10^7 plaque-forming unit (PFU)/ml). After 2 days, cells were stained with X-Gal.

Quantification of rAAV genome in canine muscle

To quantify rAAV genomes, muscle sections were digested with proteinase K, followed by phenol/chloroform extraction and isopropanol precipitation. The DNA pellet was resuspended in TE buffer, and amplified by PCR with following primer sets: 5′-ccacgctgttttgacctccatag-3′ (downstream of transcription start site in the CMV promoter) and 5′-gtacaattccgcagcttttagagc-3′ (upstream of the *LacZ* gene) for rAAV2-CMVLacZ (the PCR product is 244 bp, illustrated in Figure 1a); 5′-gcagttatctggaagat cagg-3′ and 5′-cataaccaccacgctcatcg-3′ (within the *LacZ* gene) for rAAV2-LacZ-P(−) (the PCR product is 275 bp, illustrated in Figure 4a). As an internal control, the canine calmodulin gene II (CaMII; GenBank accession no. D12622) was amplified with following primers: 5′-gagaggactcatccaaggtcacac-3′ and 5′-tcagaaaccacggcat cagg-3′. AAV vector plasmids for rAAV2-CMVLacZ or rAAV2-LacZ-P(−) were served as a quantity control for standard amplification.

RT-PCR for transgene mRNAs

Total RNA was isolated from muscle sections using RNAqueous-Micro kit (Ambion, TX, USA). Then first-strand cDNA was synthesized using First-Strand cDNA Synthesis Kit (GE Healthcare UK Ltd, Buckinghamshire, UK). mRNA of rAAV2-CMVLacZ was detected using the same primers used for genomic DNA (Figure 1a). The amplified product is 178 bp. As an internal control glyceraldehyde-3-phosphate dehydrogenase mRNA (GenBank accession no. AB038240) was amplified using the following primer set: 5′-tcatctctgctccttctgctgat-3′ and 5′-ggctagaggagccaagcagtt-3′.

Western blot analysis

Muscle extracts were prepared from rAAV-injected canine muscles, separated on 7.5% sodium dodecyl sulfate-polyacrylamide gels, and then transferred onto polyvinylidene fluoride membranes, as described previously.[8] β-Gal protein was detected by rabbit polyclonal anti-β-gal antibody (Cappel).

ELISA

ELISA were performed as described previously.[8] The microtiter plate was precoated with β-gal, rAAV2-CMVLacZ or rAAV2-LacZ-P(−), incubated with the sera from dogs, and then reacted with a 1/5000 dilution of peroxidase-conjugated rabbit anti-dog IgG (whole molecule) (Sigma). Reactivity was determined by the color reaction of 3,3′,5,5′,-tetramethylbenzidine (TMBZ).

IFN-γ release assay

Spleen cells were isolated from C57BL/6 mice or beagle dogs, which were untreated with rAAVs. Splenetic cells were dissociated physically and passed through 100 μm filters. After removal of red blood cells using 0.83% ammonium chloride buffer (Sigma), splenocytes were cultured in RPMI medium containing 10% FBS at a density of 2×10^6 cells/well in 24-well plates for 2 days in the presence of various antigens: β-gal (500 ng to 50 μg), rAAV2-CMVLacZ (1×10^8–1×10^{10} vg), ConA (5 ng to 5 μg, GE Healthcare Bio-Science) and phytohemagglutinin (50 ng to 50 μg, Sigma). The supernatant of the culture was assayed for the secretion of IFN-γ using Mouse or Canine IFN-γ Quantikine ELISA Kit (R&D Systems, Minneapolis, MN, USA). The amounts of canine or murine IFN-γ were calibrated using recombinant canine or murine IFN-γ proteins as standards, respectively, according to manufacturer's instructions. Results are given as means with standard deviation (s.d.) of three experiments. Data were first evaluated by *F*-test. When equality of variances was shown, *t*-test was used to evaluate the statistical significance. When rejected, Aspin–Welch-test was used.

Acknowledgements

We are grateful to Dr Katsujiro Sato, Dr Yasushi Mochizuki, Dr Naoko Yugeta, Dr Akiyo Nishiyama, Dr Madoka Ikemoto, Dr Michiko Wada, Ms Kazue Kinoshita, Ms Ryoko Nakagawa, Mr Satoru Masuda, Dr Masayuki Tomohiro and Dr Yoshiki Shimatsu for technical assistance. We also thank Mr Hideki Kita and Mr Shinichi Ichikawa and other staff of JAC Co. for care and management of experimental animals. This work is supported by Grants-in-Aid for Scientific Research for Research on Nervous and Mental Disorders (10B-1, 13B-1, 16B-3) and Health Sciences Research Grants for Research on Human Genome and Gene Therapy (H10-genome-015, H13-genome-001, H16-genome-003) from the Ministry of Heath, Labor and Welfare of Japan, and Grant-in-Aid for Scientific Research (B) from the Ministry of Education, Culture, Sports, Science and Technology (MEXT). A part of this work in Musashino University is supported by High-Tech Research Center Project for Private Universities: matching fund subsidy from MEXT, 2004.

References

1 Emery AEH. *Duchenne Muscular Dystrophy*, 2nd edn. Oxford University Press: Oxford, 1993.
2 Fisher KJ, Jooss K, Alston J, Yang Y, Haecker SE, High K *et al.* Recombinant adeno-associated virus for muscle directed gene therapy. *Nat Med* 1997; **3**: 306–312.
3 Yuasa K, Miyagoe Y, Yamamoto K, Nabeshima Y, Dickson G, Takeda S. Effective restoration of dystrophin-associated proteins *in vivo* by adenovirus-mediated transfer of truncated dystrophin cDNAs. *FEBS Lett* 1998; **425**: 329–336.
4 Harper SQ, Hauser MA, Dellorusso C, Duan D, Crawford RW, Phelps SF *et al.* Modular flexibility of dystrophin: implications for gene therapy of Duchenne muscular dystrophy. *Nat Med* 2002; **8**: 253–261.
5 Watchko J, O'day T, Wang B, Zhou L, Tang Y, Li J *et al.* Adeno-associated virus vector-mediated minidystrophin gene therapy improves dystrophic muscle contractile function in *mdx* mice. *Hum Gene Ther* 2002; **13**: 1451–1460.
6 Fabb SA, Wells DJ, Serpente P, Dickson G. Adeno-associated virus vector gene transfer and sarcolemmal expression of a 144 kDa micro-dystrophin effectively restores the dystrophin-associated protein complex and inhibits myofibre degeneration in nude/*mdx* mice. *Hum Mol Genet* 2002; **11**: 733–741.
7 Sakamoto M, Yuasa K, Yoshimura M, Yokota T, Ikemoto T, Suzuki M *et al.* Micro-dystrophin cDNA ameliorates dystrophic phenotypes when introduced into *mdx* mice as a transgene. *Biochem Biophys Res Commun* 2002; **293**: 1265–1272.

8 Yuasa K, Sakamoto M, Miyagoe-Suzuki Y, Tanouchi A, Yamamoto H, Li J *et al*. Adeno-associated virus vector-mediated gene transfer into dystrophin-deficient skeletal muscles evokes enhanced immune response against the transgene product. *Gene Therapy* 2002; **9**: 1576–1588.
9 Yoshimura M, Sakamoto M, Ikemoto M, Mochizuki Y, Yuasa K, Miyagoe-Suzuki Y *et al*. AAV vector-mediated microdystrophin expression in a relatively small percentage of *mdx* myofibers improved the *mdx* phenotype. *Mol Ther* 2004; **10**: 821–828.
10 Shimatsu Y, Katagiri K, Furuta T, Nakura M, Tanioka Y, Yuasa K *et al*. Canine X-linked muscular dystrophy in Japan ($CXMD_J$). *Exp Animals* 2003; **52**: 93–97.
11 Shimatsu Y, Yoshimura M, Yuasa K, Urasawa N, Tomohiro M, Nakura M *et al*. Major clinical and histopathological characteristies of canine X-linked muscular dystrophy in Japan, $CXMD_J$. *Acta Myologica* 2005; **24**: 145–154.
12 Valentine BA, Cooper BJ, Cummings JF, De Lahunta A. Canine X-linked muscular dystrophy: morphologic lesions. *J Neurol Sci* 1990; **97**: 1–23.
13 Manno CS, Arruda VR, Pierce GF, Glader B, Ragni M, Rasko J *et al*. Successful transduction of liver in hemophilia by AAV-Factor IX and limitations imposed by the host immune response. *Nat Med* 2006; **12**: 342–347.
14 Fisher KJ, Gao GP, Weitzman MD, DeMatteo R, Burda JF, Wilson JM. Transduction with recombinant adeno-associated virus for gene therapy is limited by leading-strand synthesis. *J Virol* 1996; **70**: 520–532.
15 Herzog RW, Yang EY, Couto LB, Hagstrom JN, Elwell D, Fields PA *et al*. Long-term correction of canine hemophilia B by gene transfer of blood coagulation factor IX mediated by adeno-associated viral vector. *Nat Med* 1999; **5**: 56–63.
16 Fields PA, Kowalczyk DW, Arruda VR, Armstrong E, Mccleland ML, Hagstrom JN *et al*. Role of vector in activation of T cell subsets in immune responses against the secreted transgene product factor IX. *Mol Ther* 2000; **1**: 225–235.
17 Herzog RW, Mount JD, Arruda VR, High KA, Lothrop Jr CD. Muscle-directed gene transfer and transient immune suppression result in sustained partial correction of canine hemophilia B caused by a null mutation. *Mol Ther* 2001; 4: 192–200.
18 Herzog RW, Fields PA, Arruda VR, Brubaker JO, Armstrong E, Mcclintock D *et al*. Influence of vector dose on factor IX-specific T and B cell responses in muscle-directed gene therapy. *Hum Gene Ther* 2002; **13**: 1281–1291.
19 Arruda VR, Stedman HH, Nichols TC, Haskins ME, Nicholson M, Herzog RW *et al*. Regional intravascular delivery of AAV-2-F.IX to skeletal muscle achieves long-term correction of hemophilia B in a large animal model. *Blood* 2005; **105**: 3458–3464.
20 Zhang Y, chirmule N, Gao G, Wilson J. CD40 ligand-dependent activation of cytotoxic T lymphocytes by adeno-associated virus vectors *in vivo*: role of immature dendritic cells. *J. Virol* 2000; **74**: 8003–8010.
21 Wang Z, Zhu T, Qiao C, Zhou L, Wang B, Zhang J *et al*. Adeno-associated virus serotype 8 efficiently delivers genes to muscle and heart. *Nat Biotechnol* 2005; **23**: 321–328.
22 Inagaki K, Fuess S, Storm TA, Gibson GA, Mctiernan CF, Kay MA *et al*. Robust systemic transduction with AAV9 vectors in mice: efficient global cardiac gene transfer superior to that of AAV8. *Mol Ther* 2006; **14**: 45–53.
23 Xiao X, Li J, Samulski RJ. Production of high-titer recombinant adeno-associated virus vectors in the absence of helper adenovirus. *J Virol* 1998; **72**: 2224–2232.
24 Snyder R, Xiao X, Samulski RJ. Production of recombinant adeno-associated viral vectors. In: Dracopoli N, Haines J, Korf B, Morton C, Seidman C, Seidman JG, Smith D (eds). *Current Protocols in Human Genetics*. John Wiley & Sons Ltd: New York, 1996, pp 12.1.1–12.2.23.
25 Auricchio A, Hildinger M, O'connor E, Gao GP, Wilson JM. Isolation of highly infectious and pure adeno-associated virus type 2 vectors with a single-step gravity-flow column. *Hum Gene Ther* 2001; **12**: 71–76.
26 Howell JM, Fletcher S, Kakulas BA, O'hara M, Lochmuller H, Karpati G. Use of the dog model for Duchenne muscular dystrophy in gene therapy trials. *Neuromuscul Disord* 1997; **7**: 325–328.
27 Howell JM, Lochmuller H, O'hara A, Fletcher S, Kakulas BA, Massie B *et al*. High-level dystrophin expression after adenovirus-mediated dystrophin minigene transfer to skeletal muscle of dystrophic dogs: prolongation of expression with immunosuppression. *Hum Gene Ther* 1998; **9**: 629–634.
28 Rando TA, Blau HM. Primary mouse myoblast purification, characterization, and transplantation for cell-mediated gene therapy. *J Cell Biol* 1994; **125**: 1275–1287.

Supplementary Information accompanies the paper on Gene Therapy website (http://www.nature.com/gt)

BMC Musculoskeletal Disorders

BioMed Central

Research article

Open Access

Activation and localization of matrix metalloproteinase-2 and -9 in the skeletal muscle of the muscular dystrophy dog ($CXMD_J$)

Kazuhiro Fukushima[1], Akinori Nakamura*[2], Hideho Ueda[3], Katsutoshi Yuasa[2], Kunihiro Yoshida[1], Shin'ichi Takeda[2] and Shu-ichi Ikeda[1]

Address: [1]Third Department of Medicine (Neurology and Rheumatology), Shinshu University School of Medicine, Matsumoto 390-8621, Japan, [2]Department of Molecular Therapy, National Institute of Neuroscience, National Center of Neurology and Psychiatry (NCNP), Kodaira 187-8502, Tokyo, Japan and [3]Department of Anatomy and Cell Biology, School of Health Sciences, Shinshu University, Matsumoto 390-8621, Japan

Email: Kazuhiro Fukushima - fuku@hsp.md.shinshu-u.ac.jp; Akinori Nakamura* - anakamu@ncnp.go.jp; Hideho Ueda - hueda@gipac.shinshu-u.ac.jp; Katsutoshi Yuasa - yuasa@ncnp.go.jp; Kunihiro Yoshida - kyoshida@hsp.md.shinshu-u.ac.jp; Shin'ichi Takeda - takeda@ncnp.go.jp; Shu-ichi Ikeda - ikedasi@hsp.md.shinshu-u.ac.jp

* Corresponding author

Published: 28 June 2007

BMC Musculoskeletal Disorders 2007, 8:54 doi:10.1186/1471-2474-8-54

Received: 4 February 2007
Accepted: 28 June 2007

This article is available from: http://www.biomedcentral.com/1471-2474/8/54

Abstract

Background: Matrix metalloproteinases (MMPs) are key regulatory molecules in the formation, remodeling and degradation of all extracellular matrix (ECM) components in both physiological and pathological processes in various tissues. The aim of this study was to examine the involvement of gelatinase MMP family members, MMP-2 and MMP-9, in dystrophin-deficient skeletal muscle. Towards this aim, we made use of the canine X-linked muscular dystrophy in Japan ($CXMD_J$) model, a suitable animal model for Duchenne muscular dystrophy.

Methods: We used surgically biopsied tibialis cranialis muscles of normal male dogs (n = 3) and $CXMD_J$ dogs (n = 3) at 4, 5 and 6 months of age. Muscle sections were analyzed by conventional morphological methods and *in situ* zymography to identify the localization of MMP-2 and MMP-9. MMP-2 and MMP-9 activity was examined by gelatin zymography and the levels of the respective mRNAs in addition to those of regulatory molecules, including MT1-MMP, TIMP-1, TIMP-2, and RECK, were analyzed by semi-quantitative RT-PCR.

Results: In $CXMD_J$ skeletal muscle, multiple foci of both degenerating and regenerating muscle fibers were associated with gelatinolytic MMP activity derived from MMP-2 and/or MMP-9. In $CXMD_J$ muscle, MMP-9 immunoreactivity localized to degenerated fibers with inflammatory cells. Weak and disconnected immunoreactivity of basal lamina components was seen in MMP-9-immunoreactive necrotic fibers of $CXMD_J$ muscle. Gelatinolytic MMP activity observed in the endomysium of groups of regenerating fibers in $CXMD_J$ did not co-localize with MMP-9 immunoreactivity, suggesting that it was due to the presence of MMP-2. We observed increased activities of pro MMP-2, MMP-2 and pro MMP-9, and levels of the mRNAs encoding MMP-2, MMP-9 and the regulatory molecules, MT1-MMP, TIMP-1, TIMP-2, and RECK in the skeletal muscle of $CXMD_J$ dogs compared to the levels observed in normal controls.

Conclusion: MMP-2 and MMP-9 are likely involved in the pathology of dystrophin-deficient skeletal muscle. MMP-9 may be involved predominantly in the inflammatory process during muscle degeneration. In contrast, MMP-2, which was activated in the endomysium of groups of regenerating fibers, may be associated with ECM remodeling during muscle regeneration and fiber growth.

Background

Duchenne muscular dystrophy (DMD) is the most common lethal X-linked recessive disease, presenting with progressive muscular atrophy and weakness. DMD is caused by mutations in the *DMD* gene that encodes the cytoskeletal protein dystrophin. Dystrophin and the dystrophin-associated protein complex provide a crucial structural link between the extracellular matrix (ECM) and the intracellular actin cytoskeleton [1]. Dystrophin deficiency affects the sarcolemma-ECM interaction, resulting in sarcolemmal instability [2,3]. Histopathological hallmarks in DMD include degeneration, necrosis, and insufficient regeneration of muscle fibers, suggesting that constitutive ECM remodeling takes place in DMD skeletal muscles. Although the cycles of degeneration and regeneration of muscle fibers continues throughout postnatal development, regeneration gradually slows and the balance is eventually tipped in favor of degeneration in DMD [4].

ECM is a three-dimensional network of macromolecules, and transmits signals from cells to the ECM and vice versa, mediating cell adhesion, migration, proliferation, differentiation and survival [5]. Muscle fibers are embedded in connective tissue organized into three interconnected sheaths: (1) Epimysium is a collagenous tissue that surrounds whole muscle; (2) Perimysium is smaller bundles of collagen fibers extended inward from epimysium, separates muscle fibers into fascicles or bundles; (3) Endomysium encloses the individual muscle fibers, including basal lamina, capillaries, fine nerve branches, fibroblasts, and macrophages [6]. The basal lamina, which consists of ECM components such as type IV collagen, laminin, and proteoglycans, maintains the physiological integrity of the muscle fibers and has a role in muscle fiber repair after injury or excessive exercise [7]. In the last decade, matrix metalloproteinases (MMPs) have been shown to degrade all ECM components [8]. MMPs, a group of zinc-dependent endopeptidases, are thought to play a central role in the modulation of ECM functions [9]. MMPs are commonly induced by cytokine signals as inactive zymogens (pro-forms), that require processing of a prodomain by other MMPs or serine proteinases to attain full activity. Their activities are inhibited by endogenous MMP inhibitors (tissue inhibitors of metalloproteinases; TIMPs-1, -2, -3, and -4) [10,11]. Membranous type metalloproteinases (MT-MMPs) have recently been discovered as a subgroup of membrane-anchored metalloproteinases. Membranous type metalloproteinase-1 (MT1-MMP) is associated with pro matrix metalloproteinase type 2 (pro MMP-2) and TIMP-2 to form a trimolecular complex, that activates pro MMP-2. [12-16]. Reversion-inducing-cysteine-rich protein with Kazal Motifs (RECK) is a new class of membrane-anchored inhibitor of MMP-2, matrix metalloproteinase type 9 (MMP-9), and MT1-MMP [17]. RECK has been described as a tumor and metastasis suppressor, as well as an angiogenesis suppressor and regulator of ECM integrity [18,19]. MMP activity contributes to a variety of physiological processes, such as embryonic development, organ morphogenesis, cell migration, apoptosis, angiogenesis, cartilage remodeling, bone growth, and wound healing [8,10,20]. On the other hand, loss of the exquisite regulation of MMPs leads to extensive ECM degradation, resulting in various diseases such as tumor progression or metastasis, cerebrovascular diseases, cardiovascular diseases, rheumatoid arthritis, and lung diseases. Therefore, MMP inhibitors can be useful prospective agents for the prevention and treatment of these diseases [21-27].

With respect to muscular disorders, particular attention has been paid to a subgroup of MMPs termed 'gelatinases,' comprising MMP-2 (also called gelatinase A, or 72-kDa type IV collagenase) and MMP-9 (also called gelatinase B, or 92-kDa type V collagenase). These enzymes contain three repeats of a gelatin-binding type II fibronectin domain inserted into their catalytic domain [28]. Besides gelatin, they degrade various ECM components including denatured type I, II, and III collagen, native IV and V collagen, laminin, elastin, proteoglycan, and fibronectin [28,29]. In some inflammatory myopathies, MMP-9 is expressed primarily by invading T lymphocytes, and is implicated in the pathogenesis [30-32]. MMP-2 is up-regulated in DMD skeletal muscle, and is expressed by mesenchymal fibroblastic cells [33]. Up-regulation of MMP-2 and MMP-9 has also been observed in skeletal muscle of dystrophin-deficient *mdx* mice [34,35], an animal model of DMD. Moreover, it has been reported that MMP-2 and MMP-9 are able to process beta-dystroglycan and disrupt the link between the ECM and the cell membrane via the dystroglycan complex in the skeletal muscle from DMD and sarcoglycanopathy patients [36-38].

We hypothesized that MMP-2 and/or MMP-9 might also play an important role in the pathogenesis of muscular dystrophies, involving ECM remodeling during the cycle of muscle fiber degeneration and regeneration. We evaluated the expression, activation, and immunolocalization of MMP-2 and MMP-9, as well as of regulatory molecules MT1-MMP, TIMP-1, TIMP-2 and RECK, in the dystrophin-deficient skeletal muscle of the canine X-linked muscular dystrophy in Japan ($CXMD_J$) model of DMD, which shows more prominent skeletal muscle involvement than *mdx* mice [39].

Methods

Animals

$CXMD_J$ dogs were established by insemination of beagles with the sperm of golden retriever muscular dystrophy (*GRMD*) dogs [40]. $CXMD_J$ dogs lack dystrophin in the sarcolemma of skeletal muscles and exhibit typical dys-

trophic phenotypes, as observed in DMD and *GRMD* [39,41]. We studied three normal male dogs (Beagle) at 4, 5 and 6 months of age and three age-matched $CXMD_J$ dogs. Each of the $CXMD_J$ dogs presented with typical clinical signs of muscular dystrophy: progressive muscular atrophy and weakness, and elevated serum creatine kinase (CK) levels. The tibialis cranialis muscles of control and $CXMD_J$ dogs were obtained by surgical biopsy at the General Animal Research Facility of the National Institute of Neuroscience at the National Center of Neurology and Psychiatry (NCNP, Tokyo, Japan). The samples were rapidly frozen in isopentane cooled by liquid nitrogen. The treating and care of the dogs, and all experimental procedures, were approved by the Ethics Committee for the Treatment of Laboratory Middle-Sized Animal of the National Institute of Neuroscience, National Center of Neurology and Psychiatry (NCNP) (Tokyo, Japan). All experiments were performed with appropriate measures taken for preventing unnecessary pain.

Film in situ *zymography*

To detect the localization of gelatinolytic MMP activity in skeletal muscle tissues, we performed film *in situ* zymography (FIZ) as previously described [42-48]. 6 μm-thick cryosections from frozen samples were placed on a polyethylene terephthalate base film coated with 7 μm thickness cross-linked gelatin with (FIZ-GI, Wako Pure Chemical, Osaka, Japan) or without (FIZ-GN, Wako Pure Chemical) 1,10-phenanthroline (inhibitor of MMPs, but not of other proteinases such as trypsin). The films with sections were incubated in a moist chamber for 6 hours at 37°C. Then the films were stained with Biebrich Scarlet for 4 min and rinsed for 10 min at room temperature. The degraded gelatin was not stained with Biebrich Scarlet, and areas of gelatinolytic activity were visualized as white or weakly red areas on the red background. Gelatinolysis observed on FIZ-GN films, but not on FIZ-GI films, indicated the presence of MMP activity. Gelatinolysis seen on both FIZ-GN and FIZ-GI films indicated the activity of proteases other than MMPs (such as trypsin). The application of gelatin as substrate for *in situ* zymography has the advantage that MMP-2 and/or MMP-9 have a high affinity for this substrate [49].

Histopathology and immunohistochemistry

Serial 8 μm-thick cryosections of frozen muscle were prepared and stained with hematoxylin and eosin (HE). The sections were blocked with 10% goat serum (Cedarlane Laboratories, Burlington, Canada) in PBS for 15 min and incubated at 4°C overnight with primary antibodies, followed by secondary staining. Stained specimens were mounted in Vectashield with DAPI (4', 6-diamidino-2-phenylindole, dihydrochloride) (Vector Laboratories, Burlingame, CA) for nuclear counterstaining and photographed using a fluorescence microscope BX51 (OLYMPUS, Tokyo, Japan) equipped with an air-cooled CCD camera VB-7010 (KEYENCE, Oosaka, Japan) and VB-Viewer software (KEYENCE). Primary antibodies were used as follows: rabbit anti-MMP-2 antibody (AB809, Chemicon International, Temecula, CA), rabbit anti-MMP-9 antibody (AB19047, Chemicon International), mouse anti-CD11b antibody (MCA1777S, Serotec, Oxford, UK), mouse-anti myosin developmental type heavy chain (NCL-MHCd, Novocastra, Newcastle Upon Tyne, UK), mouse anti-laminin B2 antibody (MAB1920, Chemicon International), rat anti-heparan sulfate proteoglycan, perlecan antibody (MAB1948, Chemicon International), rabbit anti-TIMP-1 antibody (sc-5538, Santa Cruz Biotechnology, Santa Cruz, CA), rabbit anti-TIMP-2 antibody (sc-5539, Santa Cruz Biotechnology), goat anti-MT1-MMP antibody (sc-12367, Santa Cruz Biotechnology), and goat anti-RECK antibody (sc-8689, Santa Cruz Biotechnology). CD11b is a leukocyte-associated antigen expressed on monocytes, macrophages, and granulocytes [50]. Myosin developmental type heavy chain (MHCd) is a myosin heavy chain isoform, present during muscle fiber regeneration, in the embryonic and neonatal periods [51].

Gelatin zymography

Frozen skeletal muscles were homogenized in an extraction buffer (62.5 mM Tris-HCl pH 6.8, 2% sodium dodecyl sulfate (SDS) 10% glycerol) and total protein content was assessed by the Bio-Rad DC Assay kit (Bio-Rad Laboratories, Hercules, CA). 100 μg of each extract dissolved in a loading buffer provided by the manufacture were electrophoresed through a gelatin-containing SDS polyacrylamide gel provided as part of the gelatin zymography kit (Gelatin Zymography kit, Yagai, Tokyo, Japan). The gel was washed with washing buffer and then incubated for 36 hours at 37°C in reaction buffer, provided by the manufacture. The gels were stained in Coomasie Brilliant Blue and destained with destain solution (Bio-Rad Laboratories). Gelatinolytic activity was identified as clear bands on a blue background. Gelatin zymography detects the activity of both active and pro-form gelatinolytic MMPs. This is because exposure to SDS during gel electrophoresis causes activation of the pro-form MMPs without proteolytic cleavage of the prodomain [52]. Quantitative results of the assays were obtained by densitometry using ImageJ v1.34s (National Institutes of Health; NIH, Bethesda, MD).

RNA isolation and reverse transcription

Total RNA was isolated from the skeletal muscles using the RNeasy fibrous tissue mini kit (QIAGEN, Hilden, Germany) and RNA quality was spectrophotometrically assessed. Reverse transcription to cDNA was performed in buffered solution containing dATP, dCTP, dGTP, dTTP, FPLC*pure* murine reverse transcriptase, RNA guard (por-

cine), RNase/DNase-free bovine serum albumin, and *Not*I-d (T) 18 primer [5'-d(AACTGGAAGAATTCGCGGCCGCAGGAAT18)-3'] according to the manufacturer's instructions, using the Ready-To-Go T-Primed First Strand Reaction Kit (Pharmacia Biotech, Brussels, Belgium).

Semi-quantitative RT-PCR

The PCR amplifications were carried out in the presence of 1.5 mM $MgCl_2$ by using standard PCR buffer, 0.2 mM dNTPs, 0.4 mM of each forward and reverse primer, 1 μl of RT products, and 0.1 units Taq DNA polymerase in a total volume of 25 μl. We designed PCR primers based on the previously published cDNAs of the canine gene sequences for MMP-2, MMP-9, MT1-MMP, TIMP-1, TIMP-2, and RECK (Table 1). 18S ribosomal RNA was used as an internal control in the semi-quantitative RT-PCR experiments. A 324 bp fragment of 18s was amplified using QuantumRNA™ Classic II 18S Internal Standard (Ambion, Austin, TX). 18S rRNA primers were mixed with competimers at an optimized ratio of 5:5 so that the signal for 18S rRNA was attenuated to the level of messages of targets by modulating the efficiency of amplification of the 18S PCR product. The PCR conditions were: initial denaturation for 1 min at 94°C; followed by 30 cycles (for MT1-MMP, TIMP-1, and TIMP-2), or 32 cycles (for MMP-9 and RECK) of 94°C for 30 sec, 60°C for 30 sec and 72°C for 30 sec; and a final extension of 10 min at 72°C. The number of cycles was determined experimentally so that semi-quantitative comparison could be made during the exponential phase of the amplification process for each target and 18S rRNA gene. The relative expression level of each target gene was calculated by normalization against the 18s rRNA level. The PCR products were electrophoresed through a 2.5% agarose gel stained with ethidium bromide. The gel images were obtained using the GENE FLASH syngene bio imaging (TopoGEN, Port Orange, FL), and the densities of the products were quantified using ImageJ v1.34s (NIH). All assays were conducted in triplicate.

Statistical analysis

Quantitative data were compared in both groups by Mann-Whitney's U test. The data are presented as mean ± SEM. $P < 0.05$ was considered to indicate statistical significance.

Results

Histopathology and in situ zymography

$CXMD_J$ muscles showed typical histopathological hallmarks of degeneration and regeneration. Multiple foci of both degenerating and regenerating muscle fibers were observed simultaneously in the same section (Fig. 1C). We examined the localization of gelatinolytic activity in the skeletal muscle of control and $CXMD_J$ dogs. In controls, low gelatinolytic activity was detected in the endomysium (Fig. 1A,B). In contrast, strong activity was detected in the endomysial space with infiltrating inflammatory cells in $CXMD_J$ muscles (Fig. 1D,E). Moreover, the endomysium of groups of regenerating fibers showed prominent gelatinolytic activity in $CXMD_J$ muscles (Fig. 1F,G).

We next examined the fibers characterized by prominent gelatinolytic activity using immunohistochemistry. Strong gelatinase activity was detected in the endomysium not only of fibers with infiltration of CD11b positive cells (Fig. 2A,B,C), but also of MHCd-positive, small caliber, centronuclear fibers (Fig. 2E,F,G), which represent degenerating and regenerating fibers, respectively. Gelatinolytic activity was attenuated by the MMP inhibitor, 1,10-phenanthrolone (Fig. 2D,H), indicating that it was specifically derived from MMPs, and not from other proteases.

Immunohistochemistry of MMP-9

In $CXMD_J$ muscle, MMP-9 immunoreactivity was detected in the necrotic fibers with inflammatory cell invasion and their endomysial space. MMP-9 immunoreactivity was co-localized with that of CD11b (Fig. 3G–J). Some MMP-9-positive fibers had degenerated and showed a weak and discontinuous immunoreactivity pattern of basal lamina components, perlecan (Fig. 3O–R) and laminin B2 (Fig. 3S–V). On the other hand, regenerating fibers (MHCd-positive fibers) in $CXMD_J$ muscle did not show MMP-9 immunoreactivity (Fig. 3K–N). Control muscle did not show a significant immunoreactivity for MMP-9, CD11b and MHCd (Fig. 3B,C and 3D, respectively), and revealed a normal immunoreactivity of perlecan and laminin B2 (Fig. 3E and 3F, respectively). Each immunohistochemistry of MMP-2, MT1-MMP, TIMP-1, TIMP-2, or RECK failed because of poor immunoreactivity of each antibody to the canine isoforms.

Gelatin zymography

We next evaluated the activity of each of the gelatinolytic enzymes (MMP-2, pro MMP-2 and pro MMP-9) in the muscle of normal and $CXMD_J$ dogs by gelatin zymography analysis. This analysis detected gelatinolytic enzyme activity associated with proteins of molecular weights corresponding to 74 kDa, 64 kDa and 92 kDa, which indicate the presence of pro MMP-2, and the active forms of MMP-2 and pro MMP-9, respectively. The activities of the three enzymes, particularly pro MMP-9, were increased in $CXMD_J$ muscle compared to control samples. MMP-9 was only detected as the pro-form (Fig. 4A). A semi-quantitative analysis showed a significant difference in each MMP activity between $CXMD_J$ and normal dog muscle (Fig. 4B).

Table 1: Primer sets used for PCR

Target gene (GenBank accession No.)	**Primer set (Location of primer sequence)**
MMP-2	Forward 5'-TGCAAGGCAGTGGTCATAGCT-3' (1724–1744)
(XM 535300)	Reverse 5'-AGCCAGTCGGATTTGATGCT-3' (1829–1810)
MMP-9	Forward 5'-CCCTGCCACTTCCCCTTCACC-3' (707–727)
(AF 001003219)	Reverse 5'-GAGCGGCCCTCGAAGGTGAAC-3' (895–915)
MT1-MMP	Forward 5'-AGGAGACAAGCACTGGGTGTT-3' (38–58)
(AF 097638)	Reverse 5'-AGGGATTCCTTCCCAGACCTT-3' (249–269)
TIMP-1	Forward 5'-CCGACTTAAACCGGCGTTAT-3' (201–220)
(NM 001003182)	Reverse 5'-GATCAACACCTGCAGTTTCG-3' (401–420)
TIMP-2	Forward 5'-CAAAGCGGTCAGTGTGAAGG-3' (1–20)
(AF 095638)	Reverse 5'-CTTTGTGACTTCATCGTGCC-3' (236–255)
RECK	Forward 5'-TGCCCCGAAACAATGGTTGA-3' (246–265)
(NM 001002985)	Reverse 5'-TCTCGGCAGTTTGTGTGATGG-3' (494–514)

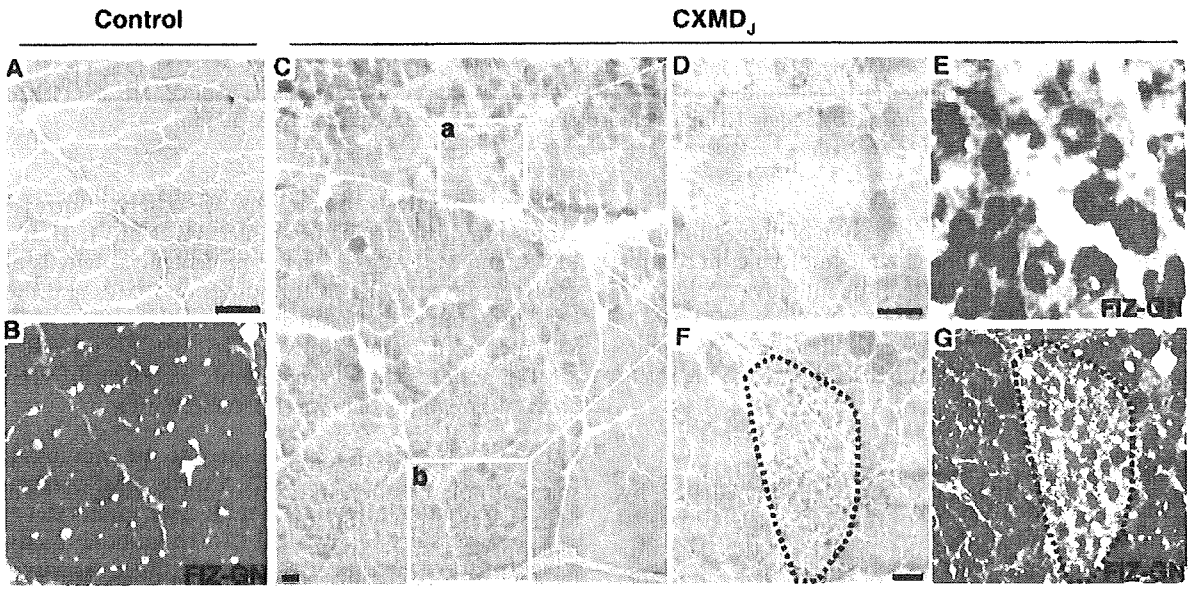

Figure 1
Film *in situ* zymography (FIZ-GN) of skeletal muscle in CXMD$_J$ dogs. Hematoxylin and eosin (H&E) staining (A, C, D, and F) and film *in situ* zymography (FIZ-GN) (B, E, and G) of the tibialis cranialis muscle in a normal dog (A, B) and a CXMD$_J$ dog (C-G). D and E (magnified views of C-a): a representative area of massive necrotic fibers with inflammatory infiltrate. F and G (magnified views of C-b): a representative area of a group of regenerating fibers. Gelatinolytic activities were visualized as white or weakly red areas on the red background. Bars, 100 μm.

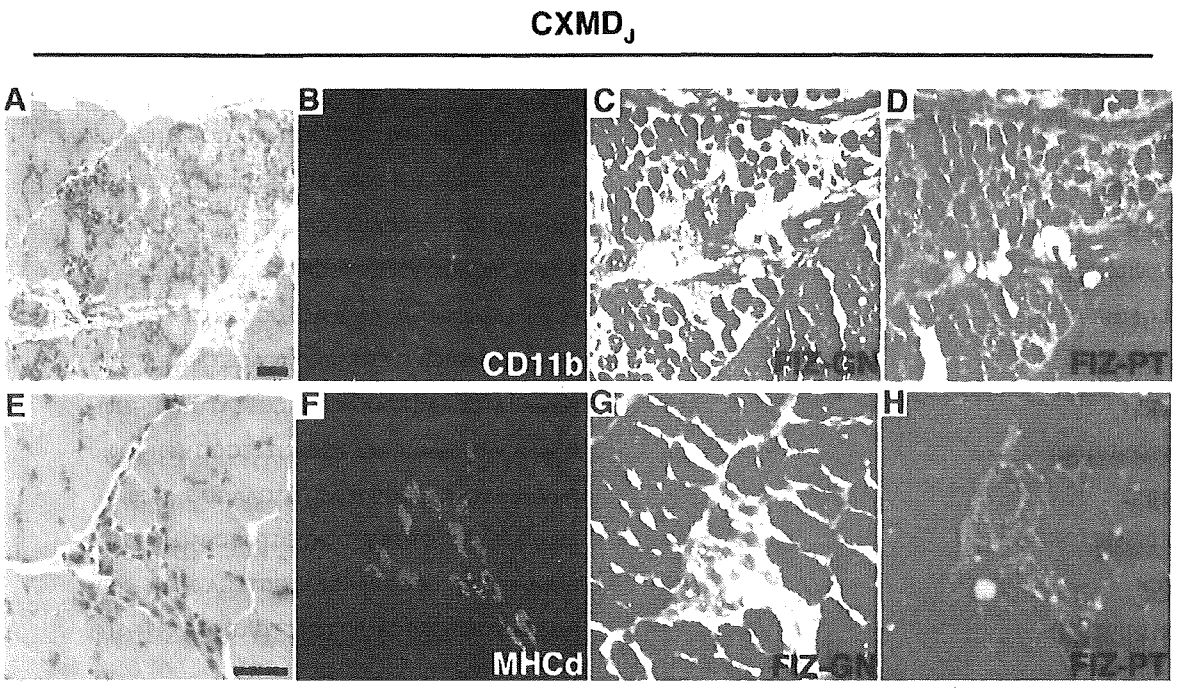

Figure 2
Immunohistochemical analysis of CD11b or MHCd expression, and film *in situ* zymography in the presence and absence of an MMP inhibitor (FIZ-PT) in the skeletal muscle of $CXMD_J$ dogs. A-D: serial sections of $CXMD_J$ muscle characterized by extensive necrosis and an invading inflammatory infiltrate; E-H: serial sections of groups of regenerating fibers in $CXMD_J$ muscle. A and B: H&E staining; B and F: immunohistochemical analysis of CD11b; C and G: FIZ-GN; D and H: FIZ in the presence of an MMP inhibitor (1,10-phenanthrolone) (FIZ-PT). Gelatinolytic activity co-localized with CD11b and MHCd, immunoreactivity and was attenuated by adding 1,10-phenanthrolone to the FIZ assay system. Bars, 50 μm.

Semi-quantitative RT-PCR

We next analyzed each gene expression of the gelatinolytic enzymes or the associated regulatory molecules in control and $CXMD_J$ dog muscle. A semi-quantitative analysis of the mRNA level encoding MMP-2, MMP-9, MT1-MMP, TIMP-1, TIMP-2, and RECK revealed that they were significantly increased in $CXMD_J$ muscle compared to the levels in control muscle (Fig. 5).

Discussion

Our data suggest that ECM remodeling mediated by MMP-2 and MMP-9 is a key process in skeletal muscle fiber degeneration and regeneration in $CXMD_J$ dogs. An FIZ assay revealed multiple foci of both degenerating and regenerating muscle fibers associated with gelatinolytic activity that was attenuated by exposure of the tissue to an MMP inhibitor, 1,10-phenanthrolone, indicating the presence of the activity of the gelatinolytic subgroup MMPs, MMP-2 and MMP-9. We also observed increased MMP-2 and MMP-9 activity and expression using gelatin zymography and by measuring the corresponding mRNAs, respectively. In addition, we observed increased expression of the regulatory molecules, TIMP-1, TIMP-2, RECK, and MT1-MMP. Overall proteolytic activity is not easily predicted by RT-PCR findings on MMPs and their regulators, but we performed FIZ to know total gelatinase activities *in situ*. Our results showed that two proteases, MMP-2 and/or MMP-9 were highly activated in certain areas, although the data was not quantitative.

We showed that MMP-9 was localized to the endomysial space of inflammation in $CXMD_J$ muscle. MMP-9 seems to be derived from infiltrating granulocytes, monocytes or macrophages, since MMP-9 and CD11b immunoreactivity appear to co-localize. Degenerating fibers associated with MMP-9 immunoreactivity exhibited weak and disconnected expression of basal lamina components, laminin B2 and perlecan. These results suggest that MMP-9 may promote the degradation of the basal lamina in necrotic fibers in $CXMD_J$ muscle, followed by inflammatory cell invasion. In cardiotoxin-injected mice, MMP-9 was induced within 24 h of injection into skeletal muscle

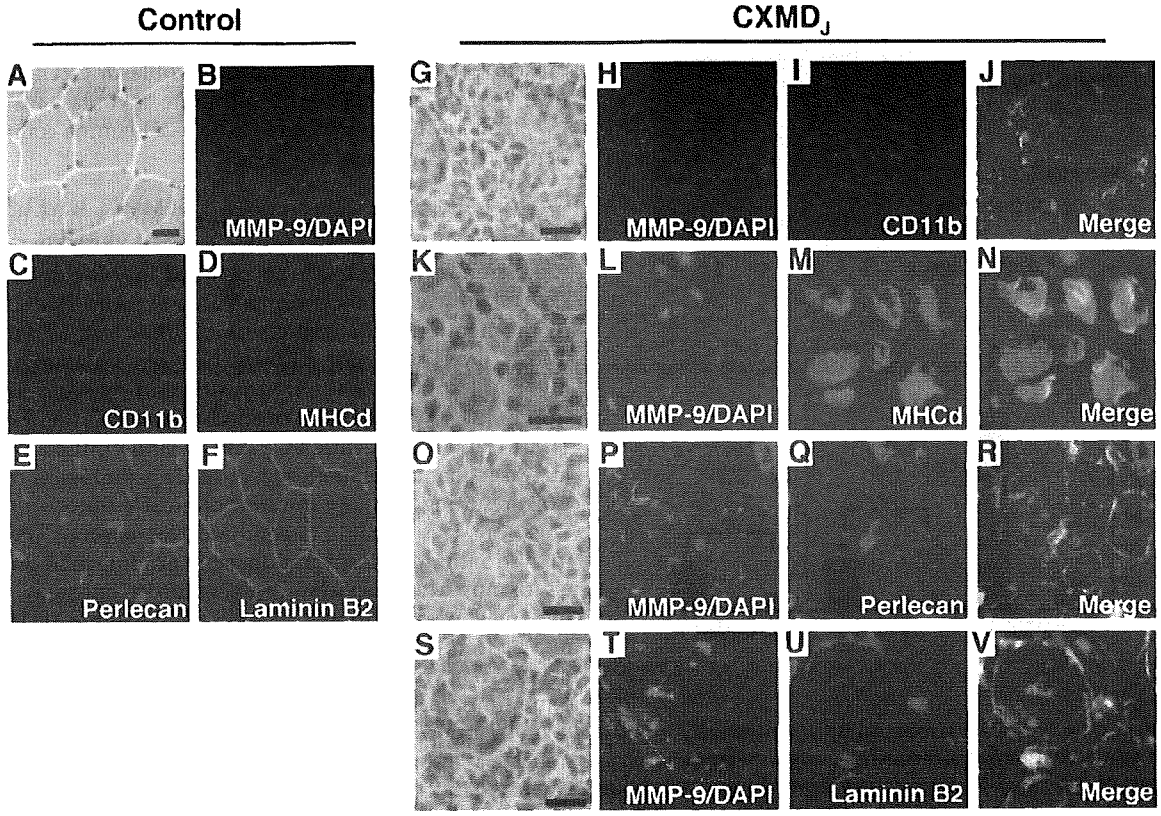

Figure 3

Co-immunolocalization of MMP-9, Perlecan, and laminin B2 in the skeletal muscle of CXMD$_J$ dogs. H&E staining (A, G, K, O and S). Immunohistochemical analysis of MMP-9 (red), with nuclear counterstain using DAPI (blue) (B, H, L, P and T), CD11b (green, C and I), MHCd (green, D and M), Perlecan (green, E and Q), laminin B2 (green, F and U). Merged images of MMP-9 immunoreactivity with that of CD11b (J), MHCd (N), Perlecan (R) and laminin B2 (V) in normal control (A-F) and in a CXMD$_J$ muscle (G-V). MMP-9 was detected in necrotic fibers associated with invading inflammatory cells and co-localized with CD11b (G-J). The endomysium of surrounding MHCd-positive regenerating fibers showed no MMP-9 immunoreactivity (K-M). A fraction of the MMP-9-positive fibers had degenerated and showed a weak and discontinuous pattern of immunostaining of both perlecan (O-R) and laminin B2 (S-V). Bars, 25 μm.

and was associated with inflammatory cell invasion, and MMP-9 mRNA was localized to invading polymorphonuclear cells and macrophages [34]. In human inflammatory myopathies, it has been reported that MMP-9 is produced primarily by invading T lymphocytes [30-32]. It is conceivable that MMP-9 may also contribute to elimination of necrotic fibers, so as to make room for muscle regeneration. MMP-9 is reported to be associated with muscle satellite cells; an adult muscle precursor and candidate muscle stem cell, and cultured human muscle satellite cells treated with phorbol ester [53]. MMP-9 mRNA was expressed in putative activated satellite cells in injured mouse muscle [34]. Taken together, these data suggest that MMP-9 might be associated not only with ECM degradation during inflammation, but also during the initiation of muscle regeneration. In our experiments, we detected only the latent form of MMP-9 (pro MMP-9) in the gelatin zymography. Regarding MMP-9, it has been reported that MMP-9 is not always detected in many tissues in vivo, although pro MMP-9 is converted to MMP-9 by various protease such as MMP-1, MMP-2, MMP-3 or plasminogen activator in vitro [54]. In addition, MMP-9 activation locally occurs in a pericellular environment by inflammatory response, leaving much of the secreted MMP in its pro-form [55].

Our data indicated that MMP-2 might be activated in the endomysium of regenerating fibers in CXMD$_J$ muscle. The

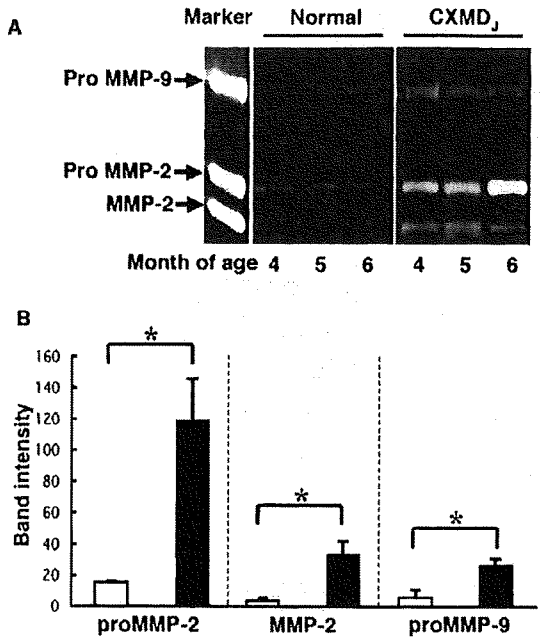

Figure 4
Gelatinolytic activities assessed by zymography in the muscle of normal and CXMD$_J$ dogs. A. Equal amounts of protein (100 μg) extracted from tibialis cranialis muscle was loaded onto a gelatin-containing SDS polyacrylamide gel. Gelatinolytic activity was identified as clear bands on a background. The activities of MMP-2, pro MMP-2 and pro MMP-9 were increased in the muscles of CXMD$_J$ dogs (n = 3) compared with those in the muscle of normal control dogs (n = 3). B. Semi-quantitative analysis of the activities of pro MMP-2, MMP-2 and pro MMP-9 in control (open bar, n = 3) and CXMD$_J$ (closed bar, n = 3) dogs based on analysis of the band intensity associated with each activity. Bar: mean ± SEM; *$p < 0.01$.

endomysium of regenerating fibers were associated with gelatinolytic MMP activity, but were not associated with MMP-9 immunoreactivity. These results suggest that MMP-2, but not MMP-9, is activated in the vicinity of regenerating fibers. In a previous report, MMP-2 transcripts were predominantly found in the areas of fiber degeneration and ECM regeneration, and were localized to mesenchymal fibroblasts in DMD skeletal muscle [33]. During muscle degeneration and regeneration induced by cardiotoxin injection, MMP-2 activity seems to be increased concomitantly with the transition from the regeneration phases characterized by the appearance of young myotubes to maturation of the myotubes into multinucleated myofibers [34,56]. We therefore, assume that MMP-2 may take part in ECM remodeling occurring in the endomysium of regenerating fibers, as they grow into mature fibers. Additionally, there are some reports indicating that MMP-2 is involved in earlier phases of muscle regeneration. In the mouse myoblastic C2C12 cell line, MMP-2 and MT1-MMP promote myoblast fusion [57], and MMP-2 could degrade the basal lamina components during myoblast fusion [40].

TIMPs, endogenous tissue inhibitors of MMPs, have been considered to be involved in the activities of MMPs. The expression of TIMPs has been explored in some diseased skeletal muscle, but their results were not conclusive. One report mentioned that expression of TIMP-1 and TIMP-2 mRNA levels were not different between inflammatory myopathies/inclusion body myositis and muscular dystrophy [32]. While, it has been also reported that both TIMP-1 and TIMP-2 mRNA levels in DMD muscle were increased than those in normal or other pathological controls, resulting in the promotion of muscle fibrosis [33]. Therefore, it is valuable to compare expression of TIMPs in dystrophin-deficiency and those in experimental models for muscle degeneration-regeneration. In our study, we presented up-regulation of TIMPs in the same skeletal muscle from CXMD$_J$ at 4 to 6 months of age, where both necrosis and regeneration was active and existed at the same time. In injured mouse skeletal muscle by cardiotoxin injection, the increase of TIMP-1 mRNA levels was noticed a little later than the peak of MMP-9 mRNA, whereas TIMP-2 mRNA levels were found corresponding to the increase in MMP-2 mRNA (Fukushima *et al.*, unpublished observations). We, therefore, suppose that MMPs and TIMPs upregulation may depend on the stage of muscle pathology; muscle necrosis or muscle regeneration, although cardiotoxin injection into canine skeletal muscle would allow us to directly compare muscle regeneration process and pathology of muscular dystrophy.

Conclusion

Based on our study, MMP-9 may be predominantly involved in the inflammatory process during muscle degeneration, while MMP-2 may be associated with ECM remodeling during muscle regeneration and fiber growth. To further elucidate the specific functions of each MMP and TIMP, canine muscle injury model by injection of a mytotoxic agent would be largely informative and therefore indispensable.

Competing interests

The author(s) declare that they have no competing interests.

Authors' contributions

KF carried out the molecular and pathological examination, and drafted the manuscript. AN participated in the design of the study and drafted the manuscript. HU per-

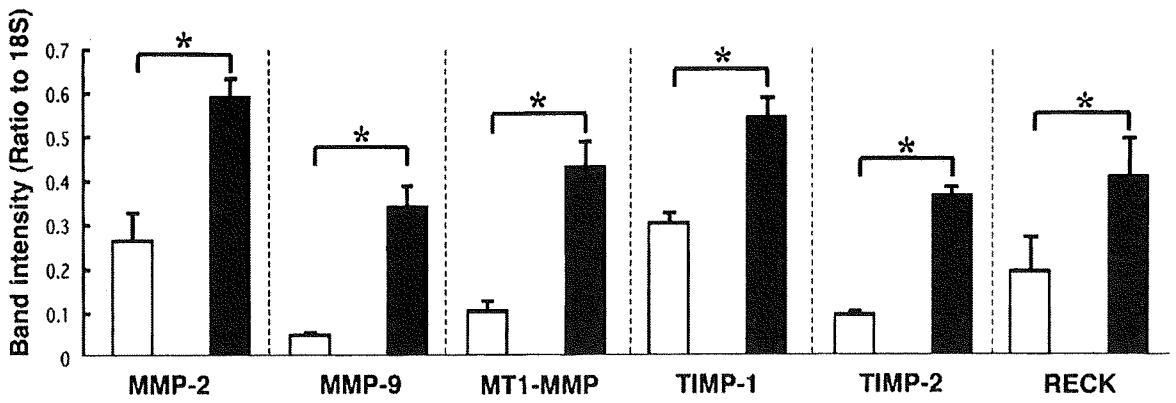

Figure 5
Relative mRNA levels of MMPs, endogenous MMPs inhibitors, and RECK in muscle from normal and CXMD$_J$ dogs. The mRNA levels of MMP-2, MMP-9, MT1-MMP, TIMP-1, TIMP-2, and RECK were examined by semi-quantitative RT-PCR. The control dogs (open bar, n = 3), CXMD$_J$ (closed bar, n = 3). Bar: mean ± SEM; *$P < 0.01$.

formed pathological analyses. KY participated in the maintenance of the dogs and necropsy. KY participated in the molecular analyses. ST participated in the design and coordination of the study. SI participated in the planning and coordination of the study. All authors read and approved the final manuscript.

Acknowledgements

We thank Naoko Yugeta, D.V.M. (School of Veterinary Medicine, Azabu University) for advising on the healthy care of dogs and also thank Hideki Kita, Shin'ichi Ichikawa, Yumiko Yahata, and Kazue Kinoshita (JAC, Inc., Tokyo) for maintaining the dogs.

This study was supported by the Research Grant for Nervous and Mental Disorders from the Ministry of Health, Labour and Welfare (17A-10), Health Sciences Research Grants for Research on Psychiatric and Neurological Diseases and Mental Health (H18-kokoro-019), the Human Genome and Gene Therapy (H16-genome-003) from the Ministry of Health, Labor and Welfare of Japan, the Grants-in-Aid for Scientific Research from the Ministry of Education, Culture, Sports, Science and Technology of Japan.

References

1. Hoffman EP, Brown RH Jr., Kunkel LM: **Dystrophin: the protein product of the Duchenne muscular dystrophy locus.** *Cell* 1987, **51(6)**:919-928.
2. Ohlendieck K, Campbell KP: **Dystrophin-associated proteins are greatly reduced in skeletal muscle from mdx mice.** *J Cell Biol* 1991, **115(6)**:1685-1694.
3. Ohlendieck K, Matsumura K, Ionasescu VV, Towbin JA, Bosch EP, Weinstein SL, Sernett SW, Campbell KP: **Duchenne muscular dystrophy: deficiency of dystrophin-associated proteins in the sarcolemma.** *Neurology* 1993, **43(4)**:795-800.
4. Blau HM, Webster C, Pavlath GK: **Defective myoblasts identified in Duchenne muscular dystrophy.** *Proc Natl Acad Sci U S A* 1983, **80(15)**:4856-4860.
5. Schenk S, Quaranta V: **Tales from the crypt[ic] sites of the extracellular matrix.** *Trends Cell Biol* 2003, **13(7)**:366-375.
6. Sans JR: **The Extracellular Matrix.** In *Myology Volume Volume 1*. 3rd edition. Edited by: Engel A FAC. New York , McGraw-Hill; 2004:471-478.
7. Carmeli E, Moas M, Reznick AZ, Coleman R: **Matrix metalloproteinases and skeletal muscle: a brief review.** *Muscle Nerve* 2004, **29(2)**:191-197.
8. McCawley LJ, Matrisian LM: **Matrix metalloproteinases: they're not just for matrix anymore!** *Curr Opin Cell Biol* 2001, **13(5)**:534-540.
9. Balcerzak D, Querengesser L, Dixon WT, Baracos VE: **Coordinate expression of matrix-degrading proteinases and their activators and inhibitors in bovine skeletal muscle.** *J Anim Sci* 2001, **79(1)**:94-107.
10. Nagase H, Woessner JF Jr.: **Matrix metalloproteinases.** *J Biol Chem* 1999, **274(31)**:21491-21494.
11. Gomis-Ruth FX: **Structural aspects of the metzincin clan of metalloendopeptidases.** *Mol Biotechnol* 2003, **24(2)**:157-202.
12. Sato H, Takino T, Kinoshita T, Imai K, Okada Y, Stetler Stevenson WG, Seiki M: **Cell surface binding and activation of gelatinase A induced by expression of membrane-type-1-matrix metalloproteinase (MT1-MMP).** *FEBS Lett* 1996, **385(3)**:238-240.
13. Strongin AY, Collier I, Bannikov G, Marmer BL, Grant GA, Goldberg GI: **Mechanism of cell surface activation of 72-kDa type IV collagenase. Isolation of the activated form of the membrane metalloprotease.** *J Biol Chem* 1995, **270(10)**:5331-5338.
14. Kinoshita T, Sato H, Okada A, Ohuchi E, Imai K, Okada Y, Seiki M: **TIMP-2 promotes activation of progelatinase A by membrane-type 1 matrix metalloproteinase immobilized on agarose beads.** *J Biol Chem* 1998, **273(26)**:16098-16103.
15. Butler GS, Butler MJ, Atkinson SJ, Will H, Tamura T, Schade van Westrum S, Crabbe T, Clements J, d'Ortho MP, Murphy G: **The TIMP2 membrane type 1 metalloproteinase "receptor" regulates the concentration and efficient activation of progelatinase A. A kinetic study.** *J Biol Chem* 1998, **273(2)**:871-880.
16. Atkinson SJ, Crabbe T, Cowell S, Ward RV, Butler MJ, Sato H, Seiki M, Reynolds JJ, Murphy G: **Intermolecular autolytic cleavage can contribute to the activation of progelatinase A by cell membranes.** *J Biol Chem* 1995, **270(51)**:30479-30485.
17. Oh J, Takahashi R, Kondo S, Mizoguchi A, Adachi E, Sasahara RM, Nishimura S, Imamura Y, Kitayama H, Alexander DB, Ide C, Horan TP, Arakawa T, Yoshida H, Nishikawa S, Itoh Y, Seiki M, Itohara S, Takahashi C, Noda M: **The membrane-anchored MMP inhibitor RECK is a key regulator of extracellular matrix integrity and angiogenesis.** *Cell* 2001, **107(6)**:789-800.
18. Sasahara RM, Brochado SM, Takahashi C, Oh J, Maria-Engler SS, Granjeiro JM, Noda M, Sogayar MC: **Transcriptional control of the RECK metastasis/angiogenesis suppressor gene.** *Cancer Detect Prev* 2002, **26(6)**:435-443.
19. Takahashi C, Sheng Z, Horan TP, Kitayama H, Maki M, Hitomi K, Kitaura Y, Takai S, Sasahara RM, Horimoto A, Ikawa Y, Ratzkin BJ, Arakawa T, Noda M: **Regulation of matrix metalloproteinase-9**